ACS NANO

www.acsnano.org

REVIEW

High-Density Lipoproteins: Nature's Multifunctional Nanoparticles

Rui Kuai,[†,‡] Dan Li,[†,‡] Y. Eugene Chen,[§] James J. Moon,[*,†,‡,∥] and Anna Schwendeman[*,†,‡]

[†]Department of Pharmaceutical Sciences, [‡]Biointerfaces Institute, and [∥]Department of Biomedical Engineering, University of Michigan, Ann Arbor, Michigan 48109, United States

[§]Cardiovascular Center, Department of Internal Medicine, University of Michigan Medical Center, 1150 W. Medical Center Drive, Ann Arbor, Michigan 48109, United States

ABSTRACT: **High-density lipoproteins (HDL) are endogenous nanoparticles involved in the transport and metabolism of cholesterol, phospholipids, and triglycerides. HDL is well-known as the "good" cholesterol because it not only removes excess cholesterol from atherosclerotic plaques but also has anti-inflammatory and antioxidative properties, which protect the cardiovascular system. Circulating HDL also transports endogenous proteins, vitamins, hormones, and microRNA to various organs. Compared with other synthetic nanocarriers, such as liposomes, micelles, and inorganic and polymeric nanoparticles, HDL has unique features that allow them to deliver cargo to specific targets more efficiently. These attributes include their ultrasmall size (8−12 nm in diameter), high tolerability in humans (up to 8 g of protein per infusion), long circulating half-life (12−24 h), and intrinsic targeting properties to different recipient cells. Various recombinant ApoA proteins and ApoA mimetic peptides have been recently developed for the preparation of reconstituted HDL that exhibits properties similar to those of endogenous HDL and has a potential for industrial scale-up. In this review, we will summarize (a) clinical pharmacokinetics and safety of reconstituted HDL products, (b) comparison of HDL with inorganic and other organic nanoparticles, (c) the rationale for using HDL as drug delivery vehicles for important therapeutic indications, (d) the current state-of-the-art in HDL production, and (e) HDL-based drug delivery strategies for small molecules, peptides/proteins, nucleic acids, and imaging agents targeted to various organs.**

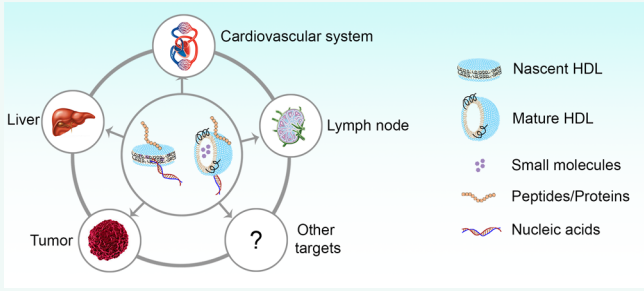

KEYWORDS: *high-density lipoproteins, apolipoproteins, apolipoprotein mimetic peptides, multifunctional nanoparticles, delivery, small molecules, peptides, proteins, nucleic acids, imaging reagents*

The discovery of high-density lipoprotein (HDL) is dated back to 1929 when a protein-rich, lipid-poor complex was isolated from equine serum at the Institute Pasteur by Macheboeuf.[1] Later in the 1950s, Eder and colleagues isolated HDL from human serum as a chemical entity by ultracentrifugation,[2] but it was not until the 1960s that the biological roles of serum lipoproteins and their impact on the cardiovascular system were suggested.[3] Today, it is well-known that HDL plays critical roles in the transport and metabolism of lipids, such as cholesterol and triglycerides.[4] Other lipoproteins involved in lipid metabolism include low-density lipoprotein (LDL), very low density lipoprotein (VLDL), and chylomicrons. Endogenous HDL is heterogeneous—possessing varying compositions and characteristics depending on its maturation stage.[5] Based on electrophoretic migration behaviors, HDL can be generally classified into three subtypes: α-migrating species, which include spherical HDL2 and HDL3; β-migrating species, which include pre-β-discoidal HDL, lipid-poor ApoA1, and free ApoA1; and γ-migrating species.[6]

The metabolic fate of HDL is described in Figure 1. The biosynthesis of endogenous HDL begins with the production of ApoA1 in the liver or intestine.[7] Nascent, discoidal HDL is then formed through lipidation of ApoA1, which is achieved through the efflux of free phospholipid and cholesterol mediated by the ATP-binding cassette transporter A1 (ABCA1) receptor. Nascent HDL is cholesterol-poor, but some cholesterol can still be found interspersed among the phospholipid molecules. Lecithin cholesterol acyltransferase (LCAT) can convert free cholesterol into cholesterol ester (CE), which can then be internalized into the core of the HDL particle, initiating its transformation from discoidal to spherical HDL. The esterification of free cholesterol is thought to form a cholesterol gradient that enables more cholesterol to bind onto the HDL surface in the subsequent steps of reverse cholesterol transport.[8] Spherical HDL can further internalize cholesterol

Received: November 28, 2015
Accepted: February 18, 2016
Published: February 18, 2016

DOI: 10.1021/acsnano.5b07522
ACS Nano 2016, 10, 3015−3041

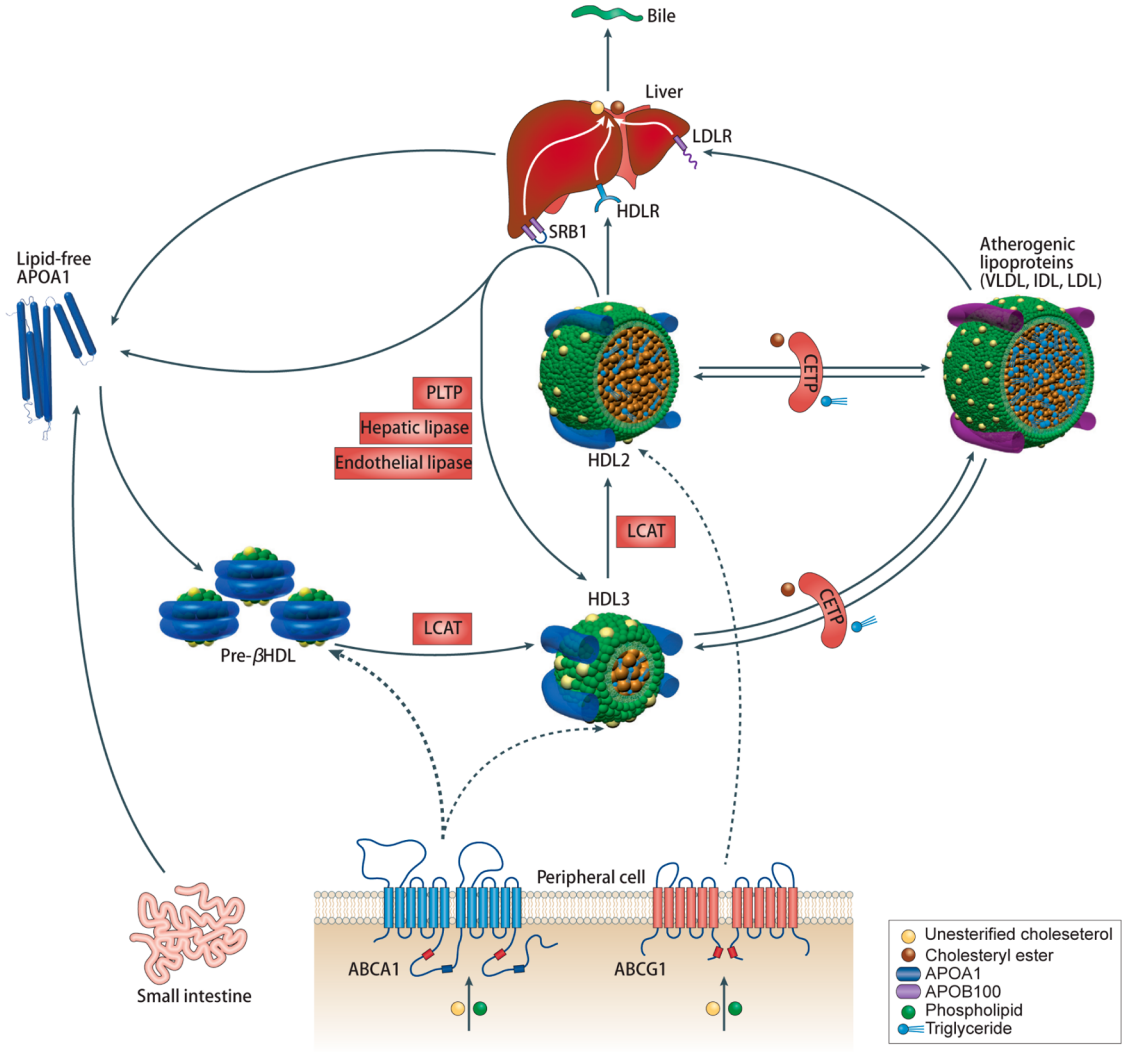

Figure 1. Metabolic fate of HDL *in vivo*. The major protein component of HDL, lipid-free ApoA1, is produced in the liver and intestine. ApoA1 can associate with lipids effluxed by ABCA1 to form nascent pre-β-HDL. The lipid layers of pre-β-HDL can be interspersed with free cholesterol, which is converted to cholesterol ester by LCAT. Cholesterol ester, which is more hydrophobic than cholesterol, is internalized into the HDL core to form spherical HDL3. Additional cholesterol from peripheral tissues can be loaded into spherical HDL3 and subsequently converted to cholesterol ester with the help of LCAT to form HDL2. Mature HDL can also exchange cholesterol ester for triglycerides from other lipoproteins such as LDL and VLDL in a process mediated by CETP. Mature HDL delivers cargo molecules to hepatocytes in the liver for metabolism through a SR-BI-mediated process. Reproduced with permission from 1. Copyright 2014 Nature Publishing Group.

effluxed by ATP-binding cassette transporter G1 (ABCG1) and scavenger receptor-type B-I (SR-BI) to become more mature, larger spherical HDL. Mature HDL can also exchange cholesterol ester for triglycerides from LDL—a process that is mediated by cholesteryl ester transfer protein (CETP). Mature HDL, which is typically composed of a hydrophobic core with cholesterol ester and triglycerides and a hydrophilic surface containing lipids and ApoA1,[8] delivers its cargo molecules to hepatocytes, where they are metabolized through an SR-BI-mediated process.[1]

HDL removes excess cholesterol from lipid-laden macrophages, called "foam cells", in atherosclerotic lesions *via* a process known as reverse cholesterol transport (RCT). HDL also possesses anti-inflammatory and antioxidative properties.[9] These functions allow HDL to exert a protective effect on the cardiovascular system, and therefore, HDL is known as "good cholesterol". Moreover, endogenous HDL is reported to transport signaling lipids, proteins, and endogenous microRNAs to recipient cells, suggesting that HDL plays multifaceted roles in complex intercellular communication.[10] These features have inspired numerous academic laboratories and pharmaceutical industries to develop HDL as delivery vehicles for various therapeutic agents. However, isolation and purification of endogenous HDL from human plasma under current good manufacturing practice (cGMP) is costly and laborious. Additionally, there are safety concerns and manufacturing challenges associated with reformulating endogenous HDL into drug-loaded therapeutics. To address these issues, various recombinant ApoA proteins and ApoA mimetic peptides have been developed within the past few years for *ex vivo* reconstitution of HDL. These synthetic HDL systems, recapitulating the *in vivo* properties of endogenous HDL, can be produced at a large scale, thus highlighting their great potential to facilitate clinical development of HDL-based therapeutics. Importantly, safety of HDL-based on ApoA proteins and ApoA mimetic

DOI: 10.1021/acsnano.5b07522
ACS Nano 2016, 10, 3015−3041

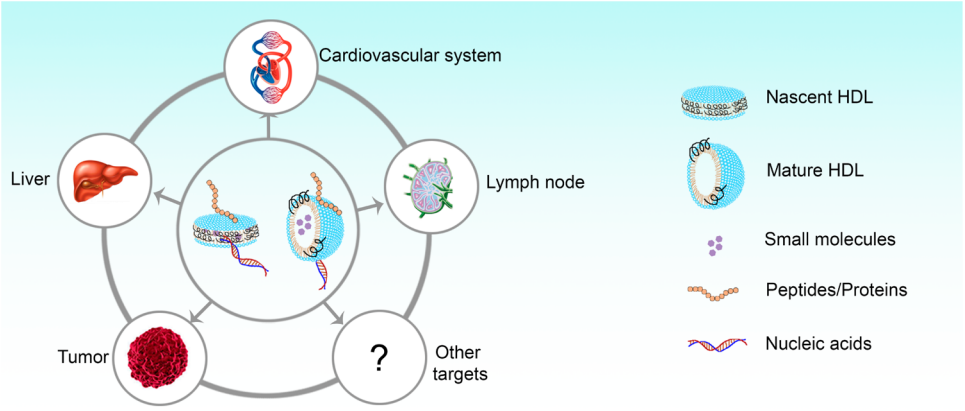

Figure 2. Delivery of different types of molecules to various target organs/tissues by HDL. HDL nanoparticles have been used to deliver small molecules, peptides/proteins, and nucleic acids to different target organs/tissues.

peptides has also been well-documented in several clinical trials at relatively high doses.[11,12]

The impact of infusion of "plain" or drug-free HDL on the cardiovascular system has been the subject of recent excellent reviews.[1,13,14] In this current review article, we will instead focus on new developments in the design and synthesis of HDL as drug delivery platforms for various biomedical applications and emphasize innovative technologies published within the last several years. We will summarize critical elements for clinical translation of nanoparticle delivery systems and the safety and pharmacokinetics data from various phase I and II clinical trials on reconstituted HDL products, which will provide the basis for future evaluation of drug-loaded HDL therapeutics. We also discuss the rationale for exploiting intrinsic tropism of HDL to specific organs and tissues as a targeted drug delivery strategy. Finally, we provide a thorough overview on the latest methods of producing both endogenous and reconstituted HDL and discuss key biomedical applications of HDL incorporated with different classes of cargo materials, including small-molecule drugs, peptides, proteins, nucleic acids, and imaging agents (Figure 2).

Critical Elements for Clinical Translation of Nano Delivery Systems. A large number of articles are published each year on nanoparticle drug delivery. Many biotechnology companies focusing on nano delivery systems are founded and financed, but most ideas never even reach phase I clinical trial. What are the scientific barriers to clinical translations, and what could be changed in the design criteria of a nanoparticle product to increase its likelihood of translational success? The first barrier is the ability to produce nanomaterials in cGMP at a scale necessary to complete toxicology and phase I clinical trials. This means that the usually rather complex chemistry of nanoparticle assembly needs to be described in a batch record and followed through step-by-step by an operator in a cGMP manufacturing plant under aseptic conditions. It also involves the development of analytical methods capable of examining concentration and purities of each component of the nano-product (*e.g.*, nanoparticle components, drug, and targeting ligand), nanoparticle size distribution, and solution safety parameters (*e.g.*, sterility, endotoxin, and osmolality). In addition, the cGMP process should be sufficiently robust and reliable for producing the same product time after time in order to fulfill the product quality specifications while assuring that the resulting product is stable for a long term (ideally >2 years). The more complex the product, the more difficult it is to fulfill the requirement for cGMP scalability. Consequently, many nanoproducts require significant effort, time, and capital to obtain the final nanomaterials ready for phase I clinical trials. In this regard, it is notable that seven different sHDL particles have reached clinical testing (Table 1), thus demonstrating the establishment of cGMP processes for sHDL products. The state-of-the-art in cGMP manufacturing of sHDL products is discussed later in this review.

The second barrier to translation is the doses: the dose required to obtain the effect (effective dose, ED), the dose at which off-target toxicity is observed (maximum tolerated dose, MTD), and the ratio of the two, also known as the therapeutic index. Individual therapeutic molecules have their respective therapeutic indexes. Incorporating drugs in nanoparticles potentially offers superior accumulation in target organ(s) and longer circulation time relative to drug solution, thus reducing the minimum therapeutically effective dose. However, nanoparticles themselves are not toxicologically inert. Depending on the size, material, and surface modifications, nanoparticles accumulate in the liver, lungs, and spleen, while hampering organ function, accelerating inflammation, and triggering immune responses.[15,16] Overall, it is critically important to consider the following parameters to determine the optimal drug−nanocarrier dose: (i) the fold enhancement in therapeutic efficacy of the nanoformulation relative to the naked drug; (ii) the therapeutic index of nanoformulation; (iii) how the formulation might be administered in a clinical setting (*e.g.*, infusion volume and frequency); and (iv) toxicity of nanoparticles themselves. While most of these parameters are specific to individual drug−sHDL formulations, safety profiles of sHDL nanocarriers have been evaluated in humans (Table 1). In these previous clinical trials, HDL nanoparticles were given as intravenous infusions at protein doses up to 50−135 mg/kg. The total administered dose of sHDL is the sum of protein and lipid dose, usually at ratios between 1:1 and 1:4.2, and the overall MTD for a 70 kg patient has been determined to be between 10 and 30 g of sHDL nanocarriers per infusion. In other words, for a drug with a hypothetical loading of as low as 5% in sHDL, it is possible to dose patients with 500−1500 mg of drug without causing adverse effect due to the nanocarrier itself. As elaborated below, these values highlight the excellent safety profile of sHDL, compared with

DOI: 10.1021/acsnano.5b07522
ACS Nano 2016, 10, 3015−3041

Table 1. Summary of Clinical Pharmacokinetics and Safety Profiles of HDL Infusions[a]

drug	composition[b]	size	clinical study	dose of ApoA1 protein or peptide	pharmacokinetics	safety	ref
SRC-rHDL (ZLB)	ApoA1/sPC (1:4.2)	7−30 nm	phase I single dose in healthy subjects (n = 7)	15 and 40 mg/kg	$T_{1/2}$ of ApoA1 > 24 h; $T_{1/2}$ of total PL ∼8 h	no major safety issues	18,19
			phase I single dose in hypercholesterolemic men (n = 24)	80 mg/kg	no data reported	no major safety issues	20
			phase I single dose in ABCA-1 heterozygotes and control subjects (n = 9)	80 mg/kg	no data reported	no major safety issues	21
CSL-111 (CSL Behring)	ApoA1/sPC (1:4.2)	7−30 nm	phase I single dose in type 2 diabetes patients (n = 7)	80 mg/kg	ApoA1 increased from 1.2 (baseline) to 2.8 g/L and returned to baseline on day 7	no major safety issues	22
			phase I single dose in patients with vascular disease (n = 20)	placebo and 80 mg/kg	llevel of HDL cholesterol increased by 20% after infusion of rHDL	no liver function changes	23
			phase I single dose in patients with type 2 diabetes (n = 13)	placebo and 80 mg/kg	$T_{1/2}$ of ApoA1 ∼68 h	no major safety issues	24
			phase I single dose in type 2 diabetes patients (n = 17)	placebo and 20 mg/kg	$T_{1/2}$ of ApoA1 ∼72 h	no major safety issues	25
			phase II multiple doses in ACS patients (n = 183)	four weekly infusions of placebo, 40 and 80 mg/kg	no report	liver function abnormalities in 80 mg/kg group; 40 mg/kg is well-tolerated	26
CSL-112 (CSL Behring)	ApoA1/sPC (1:1.5)	7−13 nm	phase I single dose in healthy subjects (n = 57)	placebo, 5, 15, 40, 70, 105, and 135 mg/kg	T_{max} of ApoA1 = 2 h; for doses >70 mg/kg; $T_{1/2}$ of ApoA1 = 14.7−99.5 h	no safety issues	27
			phase I multiple doses in healthy subjects (n = 36)	four weekly infusion of placebo, 3.4 and 6.8 g/dose; eight biweekly of 3.4 g/dose	T_{max} of ApoA1 = 2 h; $T_{1/2}$ of ApoA1 = 19.3−92.8 h	safe and well-tolerated	28,29
			phase IIa single dose in patients with stable atherothrombotic disease (n = 45)	placebo, 1.7, 3.4, and 6.8 g/dose	T_{max} of ApoA1 ≈ 2 h; $T_{1/2}$ of ApoA1 ≈ 12 h	good safety	30
			phase IIb patients with acute myocardial infarction (n = 1200)	four weekly infusions; placebo, low and medium doses	currently recruiting	currently recruiting	31
ProApoA1-liposome (UCB)	rProApoA1/sPC (1:1.25)	7−30 nm	phase I single dose in patients with low HDL cholesterol (male, n = 4)	IV infusion for 1 h or 10 min 1.6 g of proApoA1	$T_{1/2}$ of ApoA1 <24 h	no adverse events	32
			phase I single dose in FH patients (n = 4)	4 g by IV infusion over 20 min ∼40−50 mg/kg	plasma ApoA1 levels increased transiently during the first 24 h; C_{max} 64 and 35% above the baseline at 1 h, respectively	no safety issues	33

DOI: 10.1021/acsnano.5b07522
ACS Nano 2016, 10, 3015−3041

Table 1. continued

drug	composition[b]	size	clinical study	dose of ApoA1 protein or peptide	pharmacokinetics	safety	ref
ETC-216 (Esperion)	rApoA1/POPC (1:1)	7−30 nm	phase I single dose in healthy subjects (n = 32)	IV infusion of doses 0−100 mg/kg (males) and 0−50 mg/kg (females)	T_{max} of HDL free cholesterol level ≈30 min at 15 mg/kg and higher	safe and well-tolerated at all doses	34
			phase II multiple doses in ACS patients (n = 57)	five doses; once per week by IV infusion; placebo, 15 and 45 mg/kg	no report	minor gastrointestinal adverse effects in three groups; two adverse events in high-dose group deemed possibly drug-related	34,35
CER-001 (Cerenis)	rApoA1/SM/DPPG (1:2.7:0.1)	7−13 nm	phase I single dose in healthy volunteers (n = 32)	IV infusion of escalating doses of 0.25, 0.75, 2, 5, 10, 15, 30, 45 mg/kg	T_{max} of ApoA1 ≈ 1−2 h; $T_{1/2}$ ≈ 10 h; C_{max} is dose-dependent and up to 0.9 mg/dL at 45 mg/kg	safe and well-tolerated at all doses	36,37
			phase II (CHI SQUARE) multiple doses in patients with ACS (n = 507)	six weekly infusions of 0, 3, 6, and 12 mg/kg	no PK data	generally well-tolerated	38
			phase II multiple doses in patients with HoFH (n = 23)	12 biweekly infusions at 8 mg/kg	ApoA1 increased by 13% from 114.8 to 129.3 mg/dL during first hour after infusion	one serious adverse event reported to be drug-related	39,40
			phase II multiple doses in patients with FPHA (n = 7)	IV infusion for 1 h; 20 infusions at 8 mg/kg for 6 months	T_{max} of ApoA1 ≈ 4 h; $T_{1/2}$ ≈ 12 h	no serious adverse events	41
ETC-642 (Esperion)	ApoA1 peptide/DPPC/SM (1:1:1)	7−13 nm	phase I single dose in patients with stable atherosclerosis (n = 28)	IV infusion of placebo and 0.1, 0.3, 1, 3, and 10 mg/kg	dose proportional rise in the levels of peptide after infusion; $T_{1/2}$ = 8.3−12.8 h	safe and well-tolerated	11,42
			phase I single dose in patients with stable cardiovascular disease (n = 24)	IV infusion; 10, 20, 30 mg/kg	dose proportional rise in the levels of peptide; $T_{1/2}$ of peptide = 10.2−13.8 h	ssymptomatic elevations of liver function in one patient at 30 mg/kg	43
			phase I multiple doses in patients with stable cardiovascular disease (n = 32)	four weekly IV infusions of placebo 10, 20, and 30 mg/kg	no data reported	no data reported	44

[a]Abbreviations: sPC, soybean phosphatidylcholine; rApoA1, recombinant ApoA1; ACS, acute coronary syndrome; POPC, palmitoyloleoylphosphatidyl choline; SM, sphingomyelin; DPPG, dipalmitoylphosphatidyl glycerol; FH, familial hypercholesterolimea; HoFH, heterozygous familial hypercholesterolemia; FPHA, familial primary hypoalphalipoproteinemia; DPPC, dipalmitoylphosphatidylcholine. [b]Indicates weight ratio; literature reported molar ratios were converted to weight ratios.

DOI: 10.1021/acsnano.5b07522
ACS Nano 2016, 10, 3015−3041

those of other synthetic nanoformulations, thus significantly extending the potential dosing window for drug therapeutics.

Pharmacokinetics and Safety Profiles of HDL Therapeutics. A number of reconstituted HDL products have advanced to different stages of clinical trials.[17] These reconstituted HDL products (rHDL) are intended for administration following an initial cardiovascular event in patients with acute coronary syndrome (ACS) to remove excess cholesterol from arterial plaques and reduce the chance of a secondary event. The summary of clinical trials examining the doses, routes of administration, molecular composition, pharmacokinetic parameters, and safety profiles of HDL products is provided in Table 1. At least seven different HDL products have been evaluated in clinical trials, including (a) HDL based on ApoA1 purified from human plasma, such as SRC-rHDL, CSL-111, and CSL-112; (b) HDL based on recombinant ApoA1 and its variants, such as proApoA1-liposomes, ETC-216, and CER-001; and (c) rHDL based on synthetic ApoA1 mimetic peptides, such as ETC-642. The maximum tolerated doses of HDL in human patients vary depending on the composition of each product and their respective impurities. In general, the HDL products have been reported to be safe when administered once per week by prolonged intravenous infusion at up to 80 mg/kg for SRC-rHDL (~6.5 g of ApoA1/dose or 33 g of total HDL/dose), 135 mg/kg for CSL-112 (~10 g of ApoA1/dose or 35 g of total HDL/dose), 45 mg/kg for CER-001 (~4 g of ApoA1/dose or 15 g of total HDL/dose), and 30 mg/kg for ETC-642 (~3 g of ApoA1 peptide/dose or 9 g total HDL/dose). Potential safety concerns associated with HDL products include transient elevation of liver transaminases (ALT and AST) along with other minor liver toxicities. These concerns arise as a result of the hyper-pharmacology of HDL products, as a significant amount of cholesterol is rapidly mobilized from peripheral organs and delivered to the liver for metabolism. The half-life of ApoA1 in plasma following HDL administration ranges between 6 and 24 h, depending on the dose and product composition. Overall, various phase I and II clinical trials performed to date in over 800 patients and healthy volunteers have demonstrated that HDL products are well-tolerated without any major complications or severe side effects.

HDL Based on ApoA1 Purified from Human Plasma. The first rHDL product tested in a clinical trial was SRC-rHDL developed by ZLB Central Laboratory, Switzerland. ApoA1 was isolated from human plasma and reconstituted with soybean phosphatidylcholine (sPC) using the cholate dialysis process described below.[19] Nanjee *et al.* evaluated the effect of a single infusion of SRC-rHDL at 40 mg/kg in healthy volunteers.[18] The dose, up to 40 mg/kg, was safe and well-tolerated.[20,21] Following ZLB acquisition by CSL Behring, Australia, in 2000, SRC-rHDL was renamed as CSL-111. The product was tested in a large (183 patients) phase II safety and efficacy (ERASE) clinical trial in 2005.[26] Patients with ACS were administered with four infusions of CSL-111 at 40 or 80 mg/kg or placebo at weekly intervals. The high-dose CSL-111 treatment at 80 mg/kg was discontinued early due to abnormalities in liver functions, but CSL-111 was well-tolerated at the 40 mg/kg dose. Due to the safety issue, CSL-111 was reformulated into CSL-112 by reducing the lipid to protein ratio, resulting in a homogeneous particle size of 13 nm.[17] Safety of CSL-112 was evaluated in healthy volunteers following single and multiple administrations.[27] CSL-112 was found to be much safer than its predecessor, CSL-111, as higher doses up to 135 mg/kg were well-tolerated. In addition, ApoA1 levels remained above the baseline for 3 days following a single infusion of CSL-111.[28] A largest-to-date clinical trial with HDL is currently ongoing for CSL-112 in 1200 patients with acute myocardial infarction.[31]

HDL Based on Recombinant ApoA1. The first rHDL product synthesized with recombinant ApoA1 was proApoA1-liposome developed by UCB (Belgium). Pro-ApoA1, a recombinant protein produced in *Escherichia coli*, has an additional 6 amino acid pro-sequence attached to native ApoA1.[45] Pro-ApoA1 liposomes administered at 1.6 and 4 g per dose were well-tolerated, and ApoA1 levels remained elevated for over 24 h. ApoA1Milano is a naturally occurring variant of ApoA1 with Arg-173 to Cys substitution. ApoA1Milano is produced by a recombinant process in *E. coli*.[46] In 1998, Esperion acquired the rights to ApoA1Milano and produced a new rHDL product, termed ETC-216, which is composed of ApoA1Milano and 1-palmitoyl-2-oleoyl-*sn*-glycero-3-phosphocholine (POPC).[34] After five weekly infusions at 15 and 45 mg/kg, ETC-216 significantly reduced coronary plaque volume (an average of 4.2%) in treated patients measured by IVUS.[35] ETC-216 was safe and well-tolerated at all doses tested. CER-001 is another rHDL product under development by Cerenis. CER-001 is composed of dipalmitoylphosphatidyl glycerol (DPPG), sphingomyelin (SM), and recombinant human ApoA1, which is produced in a mammalian expression system in CHO cells.[38] In a phase I clinical trial in healthy volunteers, subjects were administered with escalating doses of CER-001 up to 45 mg/kg.[37] The AUC, C_{max}, and $T_{1/2}$ for ApoA1 increased with each increased dose.[37] CER-001 was also tested in a multiple-dose efficacy trial with 3, 6, and 12 mg/kg doses given once weekly for 6 weeks.[38] CER-001 was also shown to be safe and well-tolerated at all the doses tested in these trials.

HDL Based on ApoA1Mimetic Peptide. In addition to recombinant ApoA1 protein-based rHDL as described above, new rHDL systems composed of ApoA1 mimetic peptides and phospholipids have been developed. Utilization of ApoA1 mimetic peptides is expected to reduce the manufacturing cost and facilitate industrial scale-up of rHDL. ETC-642 was the first ApoA1 mimetic peptide to reach clinical evaluation.[11,43] A phase I clinical study, performed in 2002, examined a single-dose infusion of ETC-642 in 28 patients with stable atherosclerosis.[11] Study participants were monitored for 4 weeks following a single drug administration at 0.1, 0.3, 1, 3, and 10 mg/kg. As expected, the pharmacokinetics parameters, such as AUC and ETC-642 elimination half-life, increased with higher doses.[11] The second phase I trial was conducted with stable cardiovascular patients at higher doses of 10, 20, and 30 mg/kg.[43] At the highest dose level tested, evidence of asymptomatic elevations of liver functions was observed in a single patient, suggesting identification of a maximum tolerated dose. Overall, these two clinical trials have demonstrated the safety and tolerability of single infusion of ETC-642 up to 20 mg/kg dose. A multiple dose safety study with ETC-642 was also conducted at 10, 15, and 20 mg/kg doses administered once weekly for 4 weeks;[47] however, the results of this study have not yet been made public.

Comparison of HDL with Inorganic Nanoparticles and Other Conventional Organic Nanoparticles. One of the most important characteristics of HDL (both endogenous and reconstituted HDL) is its ultrasmall size, with an average diameter between 8 and 30 nm, depending on the composition and preparation method.[48] This feature is crucial, as the large surface area enables HDL to efficiently transport different cargo molecules *in vivo*. However, HDL is not the only nanoparticle

DOI: 10.1021/acsnano.5b07522
ACS Nano 2016, 10, 3015−3041

that has such ultrasmall sizes. Other inorganic nanoparticles, including gold, iron oxide, quantum dots, and silica, can also be prepared with sizes similar to that of HDL (8−30 nm).[49] By modifying these inorganic nanoparticles with different coating materials or targeting ligands, efficient delivery of cargo molecules such as peptides, proteins, and nucleic acids to target cells can be achieved.[50−53] There are several features that set apart HDL from other inorganic nanoparticles.

First, endogenous HDL transports lipids, peptides/proteins, and nucleic acids from donor cells to recipient cells *via* interaction with HDL receptors, including SR-B1, ABCA1, and ABCG1.[54,55] Composition of HDL, as determined by lipids and different Apo proteins, is crucial for the recognition of HDL by different receptors.[56] In contrast, synthetic inorganic nanoparticles lack specific endogenous receptors and cannot be recognized by the body in similar ways, despite their similarity in size. However, some recent studies showed that by coating inorganic nanoparticles with lipids and ApoA1 proteins, the hybrid nanoparticles can behave as if they are HDL nanoparticles and can even be endowed with some new properties.[57−60] For example, Cormode *et al.* reported the use of HDL for site-specific delivery of gold nanoparticles, iron oxide nanoparticles, or quantum dots for computed tomography (CT), MRI, and fluorescence imaging.[58] Briefly, gold nanoparticles, iron oxide nanoparticles, or quantum dots were coated with lipids and ApoA1 to form an HDL-like hybrid nanoparticles, with average sizes in the normal size range of HDL (7−13 nm). Control inorganic nanoparticles were coated with PEGylated phospholipids only. When these hybrid HDL nanoparticles or inorganic nanoparticles were injected into ApoE knockout mice with atherosclerosis, only hybrid HDL nanoparticles were able to efficiently accumulate in the atherosclerotic plaque, while inorganic nanoparticles failed to achieve this, although both showed similar circulation half-life *in vivo*. Moreover, confocal microscopy confirmed that HDL-coated nanoparticles, but not the control inorganic nanoparticles, were efficiently associated with macrophages that express abundant SR-BI and ABCA1/ABCG1 and efficiently interact with endogenous HDL *in vivo*.[58] These results clearly showed that HDL can achieve the site-specific delivery, while inorganic nanoparticles alone fail to do so. In addition, naked HDL without any surface modification can circulate for an extended period of time (Table 1), which is another important feature that assures that HDL can transport different molecules efficiently *in vivo*. In contrast, inorganic nanoparticles need to be modified with different coating materials such as PEG in order to be stable and circulate long enough *in vivo*.[61−63] However, such modifications with PEG may increase immunogenicity of the nanoparticles, as recently noted when repeated administrations of PEGylated liposomes were shown to elicit immunoglobulin M (IgM) responses against PEG and facilitate accelerated blood clearance (ABC) of nanocarriers.[64−67] These compounding factors may prevent optimal interaction of inorganic nanoparticles with the target cells, therefore compromising their overall delivery efficiency.[68−71]

Second, HDL, composed of lipids and Apo proteins, allows dual delivery of both hydrophobic and hydrophilic drugs. Hydrophobic molecules can be internalized or partially inserted into the core of HDL, and hydrophilic molecules can be adsorbed or conjugated to the hydrophilic surface of HDL. In addition, HDL permits differential delivery of cargo molecules and structural components of HDL. For example, several studies have confirmed that HDL can deliver its cargo molecules to target cells independent of HDL uptake.[72,73] Furthermore, HDL can also interact with SR-B1 receptors and directly deliver cargo materials to cytosol while bypassing the endosome/lysosome pathway, thus opening doors for efficient delivery of nucleic acids or other molecules that are labile in endosomal/lysosomal conditions.[74] In contrast, inorganic nanoparticles typically require surface conjugation of therapeutic molecules, and inorganic nanoparticles taken up by cells are trafficked to endosomes/lysosomes without any significant extent of recycling to cell membranes in the target cells.

Last, HDL nanoparticles have been shown to be safe and well-tolerated in numerous clinical trials. On the other hand, although inorganic nanoparticles haven been extensively studied in preclinical and clinical studies (Table 2), their potential side effects and long-term safety are still controversial. For example, Cho *et al.* reported that after intravenous injection of 13 nm PEG-coated gold nanoparticles at doses of 0.17, 0.85, and 4.26 mg/kg in mice, these nanoparticles were detected in cytoplasmic vesicles and lysosomes of liver Kupffer cells and spleen macrophages, leading to acute inflammation and apoptosis in the liver.[15] In contrast, Lasagna-Reeves *et al.* reported that following intraperitoneal injection of 13 nm gold nanoparticles at doses of 0.04, 0.2, and 0.4 mg/kg/day for 8 days, no toxicity was observed.[75] In a different study, Chen *et al.* reported that after intraperitoneal injection of 8, 12, 17, and 37 nm gold nanoparticles at a dose of 8 m/kg/week in mice, side effects including fatigue, loss of appetite, change in fur color, and weight loss were observed. Fourteen days after the injection, mice exhibited a camel-like back and crooked spine, and the majority of the mice died within 21 days.[76] However, in the same study, 3, 5, 50, and 100 nm gold nanoparticles showed no harmful side effects. These studies showed that gold nanoparticles, although generally regarded as bioinert, may cause side effects, depending on the size, composition, administration route, and dose (Table 2). While the *in vivo* toxicity of different inorganic nanoparticles is still controversial, the unaddressed long-term safety is indeed one of the greatest challenges faced by many inorganic nanoparticles, and further study is needed to address this issue.[77] In this regard, HDL is advantageous, as the components of HDL are lipids and proteins/peptides, which are completely biocompatible and biodegradable. Compared with inorganic nanoparticles, tens or even hundreds of times higher doses of HDL have been safely dosed in multiple clinical trials (Table 1). Hence, excellent safety profiles of HDL demonstrated in clinical trials should expedite translation of HDL as delivery vehicles for various therapeutics.

In addition to inorganic nanoparticles, there are many other organic nanoparticles such as liposomes, polymeric nanoparticles, and polymeric micelles that have been widely used as delivery vehicles. Their compositions, structures, physical/chemical properties, pharmacokinetic profiles, and biomedical applications have been thoroughly reviewed, and the readers are referred to these excellent reviews.[78−81] In this section, we will focus on the major differences between these conventional organic nanoparticles and HDL.

Liposomes have been widely used as delivery vehicles for several decades.[78] Their aqueous core and lipid bilayers enable convenient and efficient loading of both hydrophilic and hydrophobic cargo molecules. Some liposome formulations have been approved by the FDA and are currently commercially available for the treatment of different diseases.[78] The sizes of liposomes are typically in the range of 50−100 nm in diameter. Liposomes smaller than 50 nm are unstable and

DOI: 10.1021/acsnano.5b07522
ACS Nano 2016, 10, 3015−3041

Table 2. Preclinical/Clinical Studies of Different Types of Inorganic Nanoparticles

name	composition	preclinical/clinical study	dose/application	safety	refs
GNPs	PEG/gold NPs (13 nm)	preclinical study in mice, single dose	IV; 0.17, 0.85, and 4.26 mg/kg	acute inflammation and apoptosis in the liver	15
GNPs	gold NPs (5 nm)	preclinical study in mice and rats, single dose	IP; 0.057 for mice; 0.285 mg for rats	multiple mitoses in the liver and some foci of extramedullary hematopoiesis at 3 days after injection	16
GNPs	BSA/lysozyme, peptide/gold NPs (8−37 nm)	preclinical study in mice, multiple doses	IP; 8 mg/kg/week	fatigue, loss of appetite, change of fur color, and weight loss; camel-like back and crooked spine 14 days after injection; death of mice within 21 days	76
GNPs	gold NPs (13 nm)	preclinical study in mice, multiple doses	IP; 0.04, 0.2, and 0.4 mg/kg/day (8 days)	no evidence of toxicity was observed	75
GNPs	PEG/silica/gold nanoshell	preclinical study in rats, single dose	0.075, 0.15, 0.225, and 0.300 mg/kg	thymus mass increase and kidney mass decrease; necrosis of hepatocytes at 15 days after injection	16
gold nanoshells	PEG/silica/gold nanoshell (120 nm)	preclinical study in mice, single dose	intratumoral injection; 20−50 μL/mouse; thermal ablation of tumors	well-tolerated	89,90
gold nanoshells	PEG/silica/gold nanoshell (150 nm)	preclinical study in dogs, single dose	IV infusion; 5.2 mL/kg; thermal ablation of tumors	well-tolerated	90,91
AuroLase	PEG/silica/gold nanoshell	phase I clinical study in patients with refractory and/or recurrent tumors of the head and neck, single dose	IV infusion; thermal ablation of head/neck tumors	no evidence of systemic toxicity	92
AuroLase	PEG/silica/gold nanoshell	phase II clinical study in patients with primary and/or metastatic lung tumors, single dose	IV infusion; thermal ablation of primary and/or metastatic lung tumors	no evidence of systemic toxicity	93
CYT-6091 (Aurimune)	rhTNF/thiolyated polyethylene glycol/colloidal gold NPs (27 nm)	phase I clinical study in 30 patients with advanced or metastatic solid tumor, multiple doses	IV; 0.05 to 0.6 mg/m^2	mild and included lymphopenia, hypoalbuminemia, electrolyte disturbances, and increased plasma liver enzymes	94
Ferumoxtran-10	iron oxide/dextran T-10 (10−20 nm)	phase I clinical study in 41 healthy volunteers, single dose	IV; 0.3, 0.6, 0.8, 1.1, and 1.7 mg Fe/kg	mild to moderate adverse events in 45% subjects; no postdose change in physical exams, vital signs, or electrocardiogram	95
Ferumoxtran-10	iron oxide/dextran T-10 (10−20 nm)	phase II clinical study in 30 cancer patients, single dose	IV; 1.7 mg Fe/kg; MRI imaging	well-tolerated without major side effects	96
MFL AS1	iron oxide/aminosilane (12 nm)	phase II clinical study in 66 patients with glioblastoma, single dose	intratumoral instillation of 31.36 mg/cm^3 tumor volume; hyperthermia therapy	grade 1−3 thermal stress in six patients	97
Ferumoxsil (AMI-121)	iron oxide crystals (10 nm)	phase I clinical study in 15 healthy adult men, single dose	oral ingestion of 22.5−225 mg/dose (0.3−3 mg/kg); MRI imaging	transient diarrhea in 5 out of 15 subjects; no serious side effects observed	98

DOI: 10.1021/acsnano.5b07522
ACS Nano 2016, 10, 3015−3041

Table 2. continued

name	composition	preclinical/clinical study	dose/application	safety	refs
Ferumoxytol	iron oxide/polyglucose sorbitol carboxymethyl ether (20−30 nm)	phase II clinical study in 21 patients with chronic kidney disease (CKD), multiple doses	IV; four doses of ferumoxytol 225 mg (~3 mg/kg) every 2−3 days or two doses of 550 mg (~7 mg/kg) every week; iron replacement for chronic anemia	mild side effects including nausea, pain at the injection site, chills, and constipation in seven patients	99
Ferumoxytol	iron oxide/polyglucose sorbitol carboxymethyl ether (20−30 nm)	phase III clinical study in 750 patients with CKD, single dose	IV; 510 mg/dose (~7 mg/kg); iron replacement for chronic anemia	minor and nonspecific toxicities such as itching, site reaction, and chills; serious side effects observed in 2.9% of patients receiving ferumoxytol and 1.8% patients receiving saline placebo; acute anaphylactic reaction in one patient	100
Cornell dots	silica NPs/NIR dye/PEG/radio labeled targeting peptide (30 nm)	phase I clinical study in five patients with metastatic melanoma, single dose	IV; 3.4−6.7 nmol of Cornell dots; fluorescence and PET imaging of tumor	well-tolerated without toxic or side effects	101

impossible to prepare due to excess hysteresis on the lipid bilayer.[82] Compared with liposomes, the most striking difference for HDL nanoparticles is their ultrasmall size, typically in the range of 7−13 nm, which potentially enables HDL to better penetrate or diffuse into target organs/tissues.[83,84] In addition, liposomes without surface modifications are rapidly eliminated *in vivo*. For example, the circulation half-life of non-PEGylated liposomes is less than 30 min.[85] Although PEGylation can prolong the circulation half-life of liposomes,[86] it can negatively affect cellular uptake and intracellular delivery of cargo molecules and cause IgM-mediated accelerated blood clearance upon repeated administrations in some cases.[83] In stark contrast, HDL nanoparticles without any surface modification can mimic features of endogenous HDL and circulate for an extended period of time *in vivo* (see Table 1), while allowing delivery of cargo molecules to target cells, such as macrophages in atherosclerotic plaques, through SR-BI or ABCA1/ABCG1-mediated pathways.[54] Such key differences highlight the benefits of HDL as an endogenous drug delivery platform.

Polymeric nanoparticles such as poly(lactic-*co*-glycolic acid) (PLGA) nanoparticles have also been widely used for drug delivery because of their good biocompatibility and biodegradability. PLGA nanoparticles can be loaded with a broad range of cargo molecules and achieve controlled drug release. Similar to liposomes, PLGA nanoparticles are significantly larger than HDL and lack the long circulating and intrinsic targeting properties of HDL. In addition, unlike HDL, PLGA nanoparticles typically require PEGylation and/or surface modifications with targeting moieties for *in vivo* applications.[79] On the other hand, HDL nanoparticles lack the capacity to achieve sustained/controlled drug release profiles of PLGA nanoparticles. Thus, combining the advantages of each drug delivery system can be an attractive option to design better delivery systems. For example, Sanchez-Gaytan *et al.* recently incorporated PLGA in the hydrophobic core of HDL in order to target atherosclerotic plaque while sustaining drug release.[87] Their study showed that the sizes of PLGA−HDL hybrid nanoparticles can be tuned within the range of 30−90 nm by changing the ratio of PLGA polymer and lipids. PLGA−HDL hybrid nanoparticles exhibited properties similar to that of endogenous HDL, including their abilities for cholesterol efflux, accumulation in atherosclerotic plaques, and association with macrophages in atherosclerotic plaque. Importantly, PLGA−HDL hybrid nanoparticles mediated controlled release of cargo molecules, a unique feature that is attributed to the PLGA core. Biomimetic platforms such as these PLGA−HDL hybrid nanoparticles integrating different modules may provide novel strategies for efficient delivery and sustained release of therapeutic drug molecules in target cells/tissues.

Micelles are another category of organic nanoparticles that have been widely used for the delivery of a broad range of cargo molecules to different target cells. The sizes of micelles are in the range of 10−100 nm.[82] Although micelles can have similar sizes as HDL, they do not possess the intrinsic targeting property of HDL. For example, Cormode *et al.* reported that HDL nanoparticles loaded with a MRI imaging agent Gd-DTPA-DMPE could efficiently accumulate in atherosclerotic plaque and associate with macrophages, while micelles loaded with Gd-DTPA-DMPE could not achieve this.[88] Moreover, the disassembly of micelles is determined by the critical micelle concentration (CMC); below CMC, micelles fall apart and disassembled monomers are eliminated, thus affecting the overall drug release and pharmacokinetic profiles. In contrast,

DOI: 10.1021/acsnano.5b07522
ACS Nano 2016, 10, 3015−3041

Table 3. Summary of Different Classes of Molecules Delivered by HDL and Their Targets

category	molecules delivered by HDL	HDL composition	target	activity	particle size	refs
small molecules	statin	ApoA1/lipids	cardiovascular system	inflammation inhibition in the atherosclerotic plaques	10−30 nm	102
	sphingosine-1-phosphate (S1P)	endogenous HDL	cardiovascular system	promoting endothelial barrier function	∼10 nm	103
	Adefovir	lactosylated HDL apoproteins	liver	HBV inhibition in hepatocytes	∼11 nm	104
	amphotericin B	ApoA1/lipids	fungi	antifungal drugs	∼8.5 nm	105
	10-hydroxycamptothecin (10-HCPT)	ApoA1/lipids	tumor	anticancer drugs	∼25 nm	106
	all-trans retinoic acid (ATRA)	ApoA1/lipids	tumor	anticancer drugs	NA	107
	curcumin	ApoA1/lipids	tumor	anticancer drugs	<50 nm	108,109
	paclitaxel	ApoA1/lipids	tumor	anticancer drugs	7.4−20.7 nm	110,111
	doxorubicin	ApoA1/lipids	tumor	Aanticancer drugs	∼20 nm	112
	MPLA	ApoA1/lipids	immune system	TLR4 agonist	∼15 nm	113
peptides/ proteins	nosiheptide	ApoA1/lipids	liver	HBV inhibition in hepatocytes	<30 nm	114
	cytochrome *c*	ApoA1/lipids	tumor	anticancer drugs	20−30 nm	115
	α-melittin	ApoA mimetic peptides/ lipids	tumor	anticancer drugs	∼15 nm	116
	hemagglutinin 5 (H5)	ApoA1/lipids	immune system	protein antigens from virus	∼15 nm	117
	Yersinia pestis LcrV	ApoA1/lipids	immune system	protein antigens from bacteria	∼15 nm	118
nucleic acids	ApoB siRNA	endogenous HDL; ApoA1/ lipids; ApoE/lipids	liver	knockdown of ApoB lipoprotein	∼10 nm	72
	ApoM siRNA	endogenous HDL	liver	knockdown of ApoM lipoprotein	∼10 nm	72
	PCSK9 siRNA	ApoE/lipids	liver	LDL receptor upregulation	∼10 nm	119
	STAT3 siRNA	ApoA1/lipids	tumor	tumor growth inhibition	∼10 nm	120
	BCL2 siRNA	ApoA1 mimetic peptides/ lipids	tumor	tumor growth inhibition	∼25 nm	74
	OAT3 siRNA	endogenous HDL	brain capillary endothelial cells (BCEC)	knockdown of organic anion transporter 3 (OAT3)	∼10 nm	121
	CpG (single-stranded DNA)	ApoA1/lipids	immune system	TLR9 agonist	∼15 nm	113

as endogenous nanoparticles, HDL nanoparticles are not restricted by CMC and follow the metabolic fate of HDL *in vivo*, which is closely related to its intrinsic targeting properties as mentioned before.

Developing HDL as Delivery Vehicles Based on Its Intrinsic Targeting Properties. While previous clinical trials have mainly focused on the effect of HDL itself on the cardiovascular system, many preclinical studies have exploited the intrinsic tropism of HDL to target not only the cardiovascular system but also other organs, including the liver, tumors, and lymphoid tissues (Table 3). In this section, we will provide the rationale for HDL-based delivery of therapeutics to various target organs/tissues and discuss key examples categorized according to each target organ.

HDL and Cardiovascular System. Recent studies have shown that, during atherosclerosis, monocytes can infiltrate the plaque and subsequently differentiate into macrophages, which produce proteolytic enzymes that facilitate digestion of the extracellular matrix and plaque rupture.[122] Therefore, HDL-based delivery of anti-inflammatory therapeutics to the plaque may further improve their therapeutic efficacy, compared with the use of plain "drug-free" HDL or bolus systemic injection of drugs.[123,124] In this regard, HDL offers major advantages over other nanocarriers due to its intrinsic ability to target atherosclerotic lesions. HDL can target atherosclerotic plaques through several mechanisms.[125] First, due to severe inflammation and endothelial injury inflicted by atherosclerosis, the vasculature of atherosclerotic lesions is leaky, enabling infiltration of HDL into the intima.[126] Second, HDL can be retained in the plaque by HDL uptake in macrophages and macrophage-derived foam cells—a process mediated by the SR-BI, ABCA1, and ABCG1 receptors expressed on the surface of macrophages.[55,127] Third, cholesterol ester transfer protein may facilitate the exchange of cargo between HDL and LDL, upon which exchanged material from HDL can be delivered to the plaque through an LDL receptor-mediated process.[128] Through these non-exclusive mechanisms, HDL could either target imaging reagents to atherosclerotic plaques for diagnostic purposes or deliver therapeutic drugs to inhibit plaque growth.

HDL and the Liver. The liver, an organ that plays a vital role in metabolism, is one of the primary sites where different lipoproteins are produced. One of the most prominent cell types found in the liver is hepatocytes, which account for more than 80% of the total resident hepatic cells. Other hepatic cell types include Kupffer cells, endothelial cells, and hepatic stellate cells.[129] Notably, Kupffer cells are specialized macrophages lining the walls of the liver sinusoids that form the part of the reticuloendothelial system (RES). Kupffer cells readily phagocyte drug molecules in a nonspecific manner, leading to complete degradation of many drug molecules and loss of their therapeutic activities.[130] Hence, delivery of drugs targeted to hepatocytes, while bypassing Kupffer cells, is not an easy feat. Hepatocyte function is closely tied to the levels of LDL cholesterol, which is referred to as "bad" cholesterol. Specifically, hepatocytes can regulate the levels of LDL through secretion of ApoB, the main structural protein of LDL and modulation of

DOI: 10.1021/acsnano.5b07522
ACS Nano 2016, 10, 3015−3041

LDL receptor (LDLR) on their surface. Down-regulation of ApoB or up-regulation of LDLR on hepatocytes can reduce LDL levels and protect the cardiovascular system, thus positioning hepatocytes as the primary target for various therapeutic drugs. To achieve hepatocyte targeting, different ligands, such as galactose,[131] glycyrrhetinic acid,[132] and mannose,[133] have been used to modify proteins, polymers, and liposomes. However, the low specificity and laborious preparation methods associated with these ligands may limit their application. Several studies have evaluated the use of viral vectors, such as HBV, to efficiently deliver therapeutic molecules to hepatocytes;[134] however, safety concerns surrounding this approach, such as the potential adverse effects of viral genome insertion into patient chromosomes and immunogenicity of viral vectors, may preclude wide use of such techniques.[135]

In contrast to the use of target ligands as mentioned above, HDL has natural tropism to hepatocytes, thus offering a safe and efficient strategy for hepatocyte targeting of therapeutic molecules.[136] Specifically, HDL is taken up into hepatocytes through interaction with SR-BI receptors and delivers its cargo cholesterol ester to hepatocytes for downstream metabolism. This biological pathway therefore provides an avenue to develop HDL as a delivery vehicle for efficient transport of therapeutic drugs to hepatocytes.

HDL and Tumors. The requirements for an ideal tumor-targeted delivery system include the following: efficient accumulation in the tumor, efficient penetration/diffusion within tumor regions, and efficient intracellular delivery.[137] HDL is a promising tumor-targeted delivery system that may meet these requirements. Specifically, lipoproteins, such as HDL, are reported to circulate in the blood for an extended period of time,[138] allowing accumulation of HDL in tumor regions by the enhanced permeability and retention (EPR) effect.[73] The half-life of HDL reconstituted with ApoA1 mimetic peptides and phospholipids is approximately 15 h, which is comparable to that of PEGylated liposomes.[73] However, conventional nanoparticles, such as liposomes, are normally larger than 60 nm, which may limit a free diffusion process of nanoparticles through a dense network of extracellular matrix proteins within the tumor regions.[139] In fact, prior studies utilizing electron microscopy have revealed that the openings in the extracellular matrix of tumor cells are generally less than 40 nm.[84] On the other hand, HDL nanoparticles are typically within a diameter range of 10−20 nm, and the ultrasmall size allows HDL to penetrate and diffuse efficiently throughout tumor regions.[83] Lastly, cancer cells often require cholesterol and other membrane components for rapid proliferation.[140] Although some cancer cell types can produce cholesterol endogenously, lipoprotein-mediated transport is still the major pathway by which cancer cells acquire cholesterol.[141,142] LDL can deliver cholesterol to cancer cells *via* interaction with LDL receptors often up-regulated on cancer cells. In addition, HDL has been reported to deliver cholesterol to various types of cancer cells, including breast,[143] ovarian,[120] adrenocortical,[144] and prostate cancer cells.[145] The cholesterol delivery by HDL is believed to be mediated by SR-BI, which is responsible for the cholesterol influx to cancer cells as well as cholesterol efflux from tumor cells to HDL. As many types of cancer cells have been reported to overexpress SR-BI,[111] intrinsic recognition of SR-BI by HDL provides a good rationale for HDL-mediated targeting of drugs to cancer cells. Alternatively, tumor cells that do not express SR-BI have been targeted with HDL modified with tumor-specific ligands, such as EGF,[146] RGD,[147] and folate,[148,149] leading to improved targeting efficiency and decreased off-target side effects.

HDL and the Immune System. The immune system is a critical component to the body's ability to fight against infectious diseases and cancer.[150] In the past few years, vaccines and therapeutics targeted to the innate and adaptive immune systems have been extensively studied for prevention of infectious diseases and treatment of cancer.[151] Pattern recognition receptors (PRRs), such as Toll-like receptors (TLRs), are crucial for induction of innate and adaptive immune responses. However, the use of free TLR agonists as vaccine adjuvants has limitations, such as poor cellular uptake and unfavorable pharmacokinetic and distribution profiles, which contribute to undesirable reactogenicity and inflammatory responses *in vivo*.[152] In addition, systemic exposure to a high dose of TLR agonists may lead to cytokine storm and severe side effects.[153] Therefore, an appropriate delivery system is needed to maximize the *in vivo* efficacy of adjuvant molecules and minimize their side effects. In this regard, nanotechnology has been widely used to improve the cellular uptake and pharmacokinetic profiles of immunostimulatory agents.[154] Compared with other nanocarriers, such as polymers,[155] liposomes,[156] and PLGA nanoparticles,[157] HDL has several key advantages for activation of the immune system.[158,159] First, HDL is an endogenous, safe nanocarrier naturally produced *in vivo* with a high maximum tolerated dose. Second, HDL is stable *in vivo* even after extended exposure to serum as demonstrated by its long circulation half-life in human patients.[25,43] Third, by changing the ratio of lipids and lipoproteins, the size of HDL can be easily tuned within the range of 10−30 nm, which has been previously shown to be the optimal particle size for efficient lymph-mediated draining of nanoparticles to lymph nodes.[160] Finally, co-delivery of antigens and adjuvants to antigen-presenting cells (APCs) ensures proper activation of APCs and antigen presentation for initiation of robust adaptive immune response.[157] Whereas a simple mixture of free antigens and adjuvants leads to weak immune responses and requires high vaccine doses,[161,162] HDL with the capacity to deliver multiple classes of drugs can facilitate co-delivery of antigens and adjuvants to antigen-presenting cells. These characteristics position HDL as a promising vaccine delivery platform for activation of the immune system. However, it should be noted that endogenous HDL, when loaded with strong adjuvants such as TLR agonists, may induce self-reactive immune responses. Although this risk of autoimmune toxicities should be minimal due to central and peripheral tolerance against self-antigens found in HDL,[163,164] any use of HDL for immune activation should be carefully monitored for unintended consequences of autoreactive antibody and cellular immune responses against endogenous HDL or ApoA1-producing cells.

In addition, HDL is involved in the transport of biologically active molecules that can suppress the immune system.[165] For example, sphingosine-1-phosphate (S1P), a bioactive sphingolipid mainly carried by HDL, has been shown to suppress the immune system and may be valuable for the treatment of autoimmune diseases.[166] Therefore, depending on the cargo molecules incorporated, HDL can either potently activate the immune system to fight against infectious diseases and cancer or alternatively suppress the immune system for the prevention and treatment of autoimmune diseases. It remains to be seen how HDL-mediated transport of other biologically active

DOI: 10.1021/acsnano.5b07522
ACS Nano 2016, 10, 3015−3041

molecules impacts the immune system and how this knowledge can be exploited for improving vaccines and immunotherapies.

HDL and Other Targets. In addition to the target organs discussed above, HDL has been also reported to be selectively taken up in the gut, kidney, steroidogenic organs,[72] and brain capillary endothelial cells (BCEC).[121] Hence, it may be possible to utilize HDL for delivery of different cargo materials to these target organs, as well.

Production of HDL. While HDL has great potential to deliver different molecules to the above-mentioned targets, it is important to establish robust methods to prepare HDL with acceptable quality and quantity that meet the requirements for *in vivo* therapeutic use. In this section, we will discuss the state-of-the-art in production of different classes of HDL, including endogenous HDL isolated from plasma, HDL reconstituted with lipids and ApoA1 proteins, and HDL reconstituted with lipids and ApoA1 mimetic peptides.

Direct Isolation from Plasma. HDL can be isolated from plasma by ultracentrifugation.[167] Briefly, a one-half volume of solution with a density of approximately 1 g/mL is mixed with one volume of serum and centrifuged for 2−3 h at 340 000*g* at 16 °C. One volume of the bottom solution is mixed with a one-half volume of a solution with a density of ∼1.2 g/mL and centrifuged for 3−4 h at the same speed and temperature. Then one volume of the bottom solution is mixed with a one-half volume of a solution with a density of ∼1.5 g/mL and centrifuged again for 7−8 h at 266 000*g* at 16 °C. The HDL fraction is located in the top solution after the third centrifugation. Fast protein liquid chromatography (FPLC) has also been used to isolate HDL from the plasma.[168] Although these methods allow for the preparation of relatively pure HDL, they are very costly, time-consuming, and, therefore, suboptimal for the large-scale production of HDL.

Sodium Cholate Dialysis Method. In addition to the direct isolation of an HDL fraction from plasma, HDL can be reconstituted *in vitro* using lipids together with either ApoA1 proteins, ApoE proteins, or their mimetic peptides. Briefly, the lipid mixture (typically composed of phospholipid, cholesterol, and cholesteryl oleate) is dried under nitrogen flow to a thin film. Lipids are hydrated in buffer using sodium cholate, and an appropriate amount of ApoA1 or mimetic peptide is added. The mixture is incubated for 12 h at 4 °C, followed by dialysis against PBS for 2 days with three buffer changes to remove sodium cholate. A previous report has shown that less than 2% of the sodium cholate remains in the final synthetic HDL formulation based on the ^{3}H cholate analysis.[110] Reconstituted HDL has the size, shape, and targeting properties similar to endogenous HDL. Cholate dialysis method has been used to prepare clinical supplies for CSL-111 and CSL-112.[19]

Sonication Method. Lipid mixture (typically composed of phospholipid and cholesteryl oleate) in chloroform is dried under nitrogen flow and then placed in a vacuum oven for 1 h. PBS buffer is added to the film, and the mixture is vortexed for 5 min, followed by sonication for 60 min at 48 °C under nitrogen. ApoA1 or the mimetic peptide in PBS buffer is added to the mixture, which becomes transparent immediately. The resulting heterogeneous HDL needs to be filtered by 0.2 μm membrane and then purified by gel filtration chromatography to obtain homogeneous HDL.[146] Reconstituted HDL also has the size, shape, and targeting properties similar to those of endogenous HDL.

Single-Step Reconstitution of HDL Using Microfluidics. Even though the sodium cholate dialysis method and sonication method allow for reconstitution of HDL possessing properties similar to endogenous HDL isolated from plasma, the preparation process is lengthy and difficult to scale up. To address these issues, microfluidics has been recently used for the preparation of HDL.[169] Briefly, phospholipids dissolved in organic solution were injected into an inlet channel of a microfluidic device with a programmable syringe pump. ApoA1, dissolved in aqueous solution, was injected in the outer channels. The microfluidic device allows for rapid and effective mixing of the solution by generating tunable dual microvortices and a focusing pattern at Reynolds number (Re) of ∼150. Self-assembly of HDL was initiated with the transition of lipids from an organic solution to an aqueous solution, permitting incorporation of ApoA1 to the nascent lipid aggregates and formation of small HDL nanoparticles. HDL prepared using this method has properties similar to those of endogenous HDL.[169]

Thermal Cycling Method. Large-scale production of HDL under cGMP conditions is crucial for translation of HDL to clinical trials. Dasseux *et al.* reported a thermal-cycling-based method which can be easily used to produce HDL under cGMP conditions.[36] Briefly, lipids were weighed and added to the buffer and then dispersed at 50 °C using a high-performance disperser. The lipid suspension was then combined with ApoA1 protein or ApoA1 mimetic peptide solution and heated to 57 °C under nitrogen, followed by cooling to room temperature to form homogeneous HDL. HDL nanoparticles prepared with this method have also been shown to exhibit properties similar to those of endogenous HDL.[56] In addition, the thermal cycling method does not require costly preparation processes or organic solvent and, therefore, can be easily adapted for large-scale production of HDL.

Delivery of Various Classes of Molecular Therapeutics by HDL. *Delivery of Small Molecules.* Early in the 1970s, Rudman *et al.* demonstrated that lipophilic molecules with partition coefficients over 11 were associated with lipoproteins,[170] including HDL, which provided direct evidence that HDL may be used for the delivery of lipophilic or amphiphilic molecules.[171] Incorporation of lipophilic drugs into HDL can improve the therapeutic efficacy and reduce the side effects by enhancing the drug solubility, circulation half-life, and distribution profile.

Statins are inhibitors of 3-hydroxy-3-methylglutaryl coenzyme A reductase (HMGR) that can up-regulate LDL receptor expression in hepatocytes and, therefore, lower the level of "bad" cholesterol LDL-c.[172] Studies have also confirmed that statins may have inhibitory effects on inflammatory cells,[173] which are therapeutic targets within atherosclerotic plaques.[174] Even though reduced plaque formation was observed with extremely high doses of oral statin therapy in an atherosclerotic mouse model, such high doses are not feasible in humans due to the resulting severe side effects such as hepatoxicity and myopathy.[175] Duivenvoorden *et al.* addressed this issue by loading statin into reconstituted HDL prepared with lipids and ApoA1 protein.[102] Compared with low doses (15 mg/kg statin) of orally ingested statins, which had little to no systemic circulation due to the biotransformation in the liver, the same doses of statin−HDL formulation (15 mg/kg statin, 10 mg/kg ApoA1) exerted stronger inhibitory effects on inflammatory cells in the plaque and reduced the thickness of the vessel wall. This was attributed to the higher statin payload that entered the systemic circulation and accumulated in the plaque after statin−HDL administration (Figure 3B). In addition, 1 week high dose

DOI: 10.1021/acsnano.5b07522
ACS Nano 2016, 10, 3015−3041

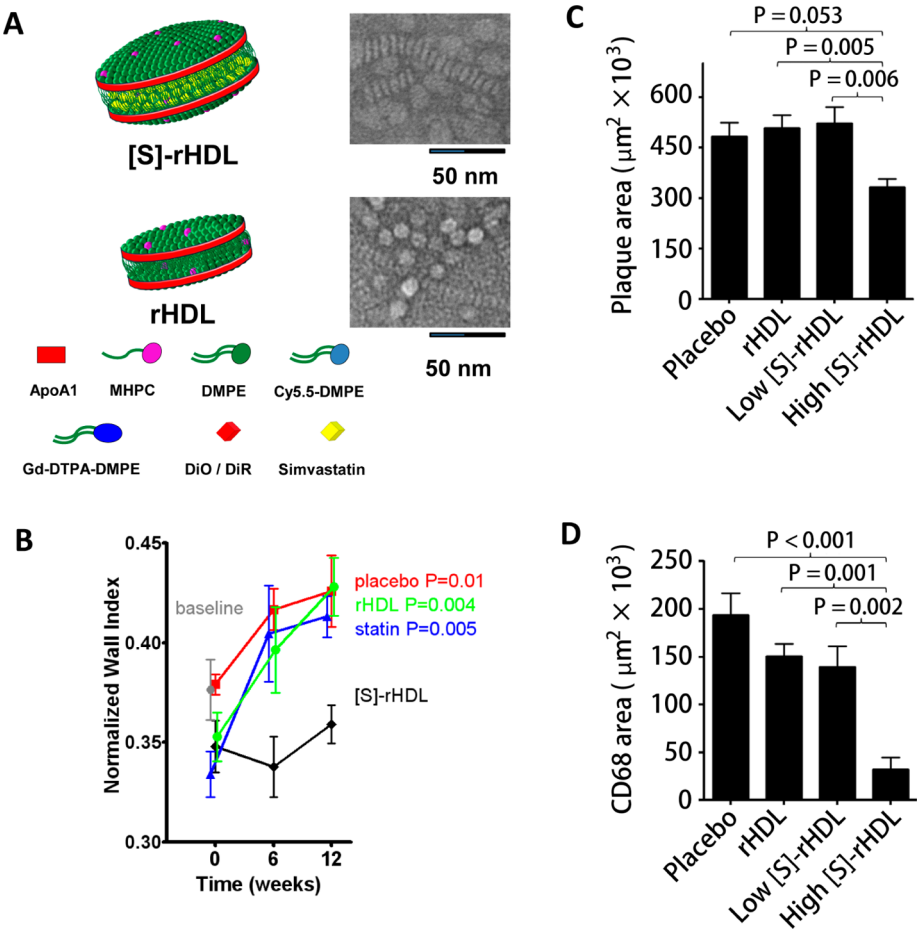

Figure 3. Delivery of statin to the atherosclerotic plaque using HDL. (A) Schematic of Simvastatin-loaded rHDL [S]-rHDL and blank rHDL (rHDL). (B) Thickness of the vessel wall of ApoE-KO mice receiving 12 weeks of biweekly low-dose [S]-rHDL (15 mg/kg statin, 10 mg/kg ApoA1), blank rHDL, statin (15 mg/kg statin), and placebo. The thickness of the vessel wall is defined as the ratio between the mean wall area and the outer wall area, which is expressed as normalized wall index (NWI). (C) Plaque area of mice receiving different formulations. High-dose [S]-rHDL (60 mg/kg statin, 40 mg/kg ApoA1) led to smaller plaque area than placebo, blank rHDL, and low-dose [S]-rHDL (15 mg/kg statin, 10 mg/kg ApoA1). (D) Plaque macrophage content (CD68-positive area) of mice receiving different formulations. High-dose [S]-rHDL significantly decreased the macrophages in the plaque compared to placebo, blank rHDL, and low-dose [S]-rHDL. Figures combined and reproduced with permission from ref 102. Copyright 2014 Nature Publishing Group.

(60 mg/kg statin, 40 mg/kg ApoA1) statin−HDL treatment was better able to reduce the plaque size and inflammatory cells than blank HDL, orally ingested statin, or low-dose statin−HDL treatment (Figure 3C,D).

9-(2-Phosphonylmethoxyethyl)adenine (PMEA; adefovir) is a promising candidate drug for inhibiting replication of hepatitis B virus (HBV) *in vitro* and *in vivo*.[176,177] However, there is minimal *in vivo* uptake of PMEA by hepatocytes, which are the primary sites of HBV infection.[178] In order to increase the delivery of PMEA to hepatocytes, De Vrueh *et al.* attached lithocholic acid-3α-oleate *via* an acid-labile bond to PMEA (PMEA-LO) and formulated it into lactosylated reconstituted HDL (LacNeoHDL) for enhanced interaction with asialoglycoprotein receptor expressed on hepatocytes.[104] Their study showed that 30 min after intravenous injection of [^{3}H]PMEA-LO-loaded LacNeoHDL (10−20 μg of [^{3}H] PMEA/kg of body weight) to rats, up to 68.9 ± 7.7% of the administered dose of [^{3}H] PMEA-LO-loaded LacNeoHDL was in the liver, whereas less than 5% of the administered dose of free [^{3}H] PMEA was in the liver. Moreover, 88.5 ± 8.2% of [^{3}H] PMEA-LO-loaded LacNeoHDL was taken up by hepatocytes. This uptake could be inhibited by 75% with asialofetulin (a substrate specific for the asialoglycoprotein receptor), indicating that the uptake process was mediated by this receptor. They also confirmed that the acid-labile bond was stable at physiological pH and was cleaved at lysosomal pH. This pH-responsiveness allowed conversion of the prodrug to the active form and thus mediated its release to the cytosol, as evidenced by subcellular fractionation. However, their study did not include drug-free HDL alone as a control group; therefore, targeting of hepatocytes with plain HDL *via* the SR-BI-mediated pathway remains to be tested in this system.

10-Hydroxycamptothecin (10-HPCT) is a potent topoisomerase-II inhibitor anticancer drug,[179] but its poor water solubility, short half-life, and severe side effects limit its use.[180] Zhang *et al.* addressed these issues by loading 10-HPCT into HDL reconstituted with lipids and the ApoA1 protein mutant, ApoA1Milano.[106] Their study showed that 10-HPCT was loaded into HDL with a drug loading of 4.31%. 10-HPCT-loaded HDL had a size of 22.4 ± 10.3 nm, which is larger than that of endogenous HDL nanoparticles. A sustained release of 10-HPCT from HDL was observed, and its release rate was slower than that of a liposome formulation. When BALB/c mice were intravenously injected with either 10 mg/kg free

DOI: 10.1021/acsnano.5b07522
ACS Nano 2016, 10, 3015−3041

HCPT or rHDLM−HCPT in PBS, rHDLM−HCPT formulation dramatically increased the concentration of 10-HPCT in major organs, compared with the free 10-HPCT, which may be due to the improved stability and circulation half-life of rHDLM−HCPT *in vivo*. Moreover, HDL formulation increased the cytotoxicity of 10-HPCT by 70 and 50 times in SKOV-3 and HCT-116 cells, respectively, *via* efficient SR-BI receptor-mediated intracellular delivery of anticancer drugs. However, *in vivo* efficacy of these formulations has not been evaluated.

HDL is an ideal carrier for lipid-like molecules. For example, endogenous HDL is reported to be involved in the delivery of bioactive lipids such as sphingosin-1-phosphate *in vivo*.[103,166] In addition to beneficial effects of HDL-S1P on the cardiovascular system, including nitric oxide production, vasodilation, and cardioprotection,[181] it was recently found that HDL-S1P can suppress lymphopoiesis by activating $S1P_1$ receptor on bone marrow lymphocyte progenitors.[166] It is believed that S1P associates with endogenous HDL *via* interaction with ApoM protein present on HDL. Using a murine autoimmune encephalomyelitis model (EAE model), the authors have shown that mice lacking ApoM developed more severe autoreactive symptoms, characterized by increased lymphocyte counts in the central nervous system and breakdown of the blood brain barrier (BBB), while overexpression of ApoM led to increased HDL-S1P and less severe autoimmune symptoms, suggesting the immunosuppressive effect of HDL-S1P on lymphopoiesis. This study underscored the potential of HDL-S1P-based therapeutics for treatment of autoimmune diseases.

Monophosphoryl lipid A (MPLA) is also a lipid-like molecule, and it can activate the innate immune system by interacting with the TLR4 receptor expressed on antigen-presenting cells. Weilhammer *et al.* formulated MPLA into HDL prepared with lipids and recombinant ApoA protein.[113] Their study showed that incorporation of MPLA into HDL dramatically potentiated the immunostimulatory effects of MPLA, as evidenced by an increase in cytokine production and up-regulation of immunoregulatory genes *in vivo*, compared with free soluble MPLA.

Other examples of HDL-based strategies for delivery of small molecules include amphotericin B,[105] all-trans retinoic acid,[107] curcumin,[108,109] paclitaxel,[111] and doxorubicin,[112] and in each case, HDL formulation improved the efficacy of the drug while decreasing its off-target side effects.

Delivery of Peptides/Proteins. Many proteins/peptides with potent biological activities are promising biotherapeutics for treatment of human diseases, but the major challenge for their wide *in vivo* use is their susceptibility to proteolysis, denaturation, and aggregation.[182] Therefore, appropriate delivery systems are needed to both protect and increase the efficacy of therapeutic peptides/proteins.[183] HDL is a nanocarrier with many advantageous properties that can potentially address these problems. There are a number of endogenous proteins and peptides that are carried on HDL, including paraoxonase, a-1-antiprypsin, serum amyloid A, and many others.[47,184] In this section, we will discuss the latest developments in HDL-based delivery of therapeutic proteins/peptides.

Direct Incorporation of Lipophilic Peptides into HDL. Nosiheptide, produced by *Streptomyces actuosus*,[185] is a lipophilic peptide and has significant anti-HBV activity in cell culture. However, limited delivery of free nosiheptide to the liver has been one of the obstacles for its clinical development. To improve its hepatocyte targeting, Feng *et al.* formulated nosiheptide into HDL reconstituted with ApoA1 and phosphotidylcholine.[114] Their study showed that the optimized HDL formulation had a drug-loading efficiency greater than 80% and a diameter smaller than 30 nm. The concentration of nosiheptide in HDL needed to achieve 50% virus inhibition (IC_{50}) in HepG2 cells *in vitro* was 40 times lower than that in control liposomes and 200 times lower than that of free nosiheptide. In addition, they found that, 30 min after i.v. injection of nosiheptide−HDL (0.5 mg/rat in 1 mL) in male Wistar rats, more than 70% of nosiheptide−HDL formulation was targeted to the liver, in comparison to less than 20% for free nosiheptide. These results clearly indicate that reconstituted HDL is a promising drug delivery platform for improving the hepatocyte targeting of lipophilic peptides.

Conjugation of Peptides/Proteins to Hydrophobic Peptide Sequence. In order to incorporate hydrophilic protein cytotoxic cytochrome *c* (cytC), an inducer of cancer cell apoptosis, and green fluorescent protein (GFP) into HDL, Kim *et al.* conjugated these proteins to membrane-permeable sequences (MPS, HAAVALLPAVLLALLAK).[115] When the protein−MPS conjugates were incubated with HDL prepared with the sodium cholate method, these proteins were incorporated into the bilayer of HDL, composed of lipids and ApoA1. The loading efficiencies of MPS−GFP and MPS−cytC were *ca.* 70 and 64−75%, respectively. In addition, anisamide (AA) was used as a targeting ligand to decorate HDL in order to further improve the efficiency of targeting tumor cells. Transition electron microscopy (TEM) revealed that 20−30 nm nanoparticles were formed. MPS−cytC was efficiently delivered by HDL into tumor cells, leading to increased cell apoptosis, as determined by confocal laser scanning microscopy (CLSM) and flow cytometry. Moreover, MPS−cytC incorporated into HDL accumulated more efficiently in tumor regions of H460-tumor-bearing mice than free cytC, as shown by the optical imaging study. When cytC (40 μg/kg) or MPS−cytC in HDL (160 μg/kg) was injected to an H460 xenograft mouse model every other day, MPS−cytC in HDL achieved higher tumor growth inhibition *in vivo*, compared with the free cytC or the physical mixture of cytC and HDL (Figure 4).

Fusion of Peptides/Proteins to ApoA1 Mimetic Peptide. Melittin, a potent cytolytic peptide, is a promising candidate for overcoming tumor drug resistance.[186] However, it has severe side effects, including hemolysis.[187] To achieve more selective targeting of melittin to tumor cells without side effects, Huang *et al.* fused the N-terminus of melittin to the C-terminus of an amphipathic ApoA1 mimetic α-helical peptide (α-peptide) *via* a GSG linker.[116] The fusion enabled melittin to interact with phospholipids and self-assemble into HDL-like nanoparticles (α-melittin-NP) with a diameter of about 20 nm. The interaction between melittin and phospholipids masked the positive charge of melittin, therefore reducing the side effect of hemolysis and increasing the maximum tolerated dose. After cellular uptake, melittin was released into cytosol and exerted its cytotoxic effect, as evidenced by confocal microscopy (Figure 5B). When B16F10-tumor-bearing mice were injected with α-melittin-NP (20 mg/kg), blank α-peptide-NPs (at the same molarity as the α-melittin NPs), or PBS, α-melittin-NP led to more efficacious tumor growth inhibition, compared with the PBS and blank HDL groups (Figure 5C).

Conjugation of Peptides/Proteins to Phospholipids. Peptide/protein antigens are attractive surrogates for live, attenuated, or killed vaccines due to their safety and relative simplicity of product manufacturing. Moreover, each component of peptide/protein antigens can be individually purified

DOI: 10.1021/acsnano.5b07522
ACS Nano 2016, 10, 3015−3041

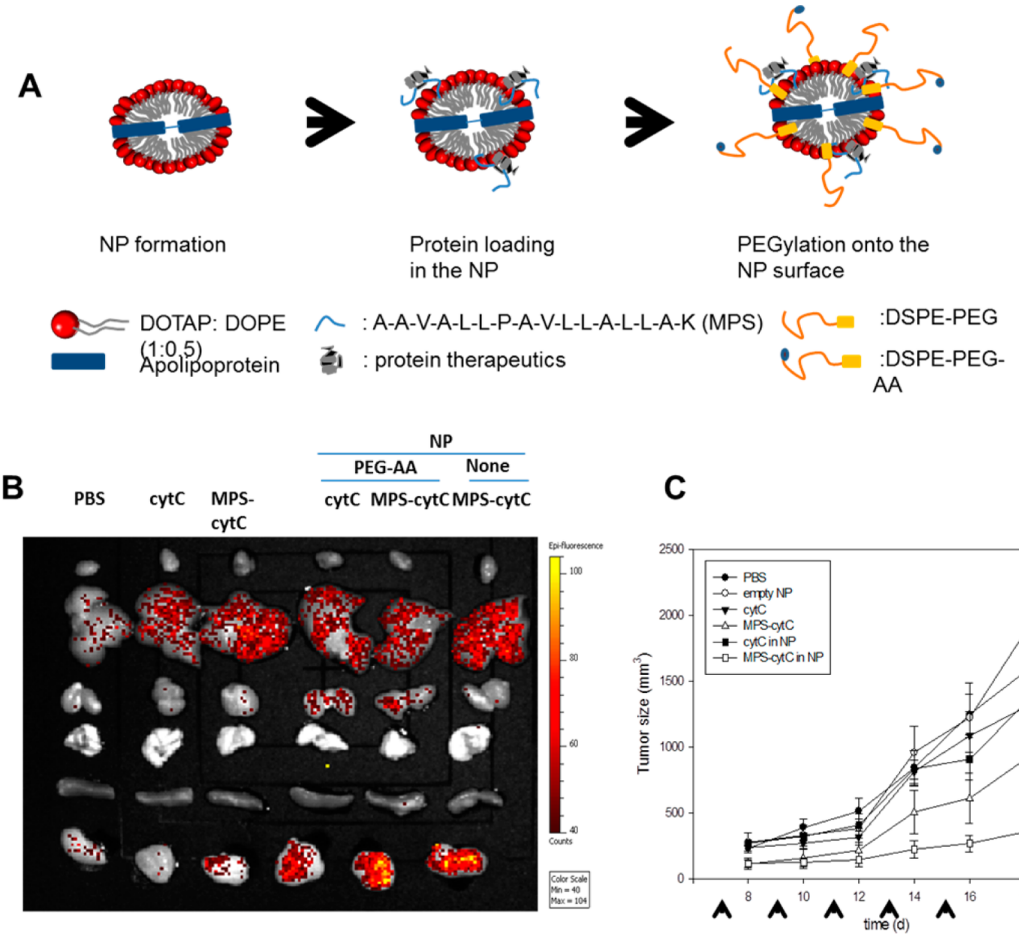

Figure 4. Increased delivery of cytotoxic cytochrome *c* to tumor cells using HDL. (A) Schematic for the preparation of protein (cytC)-loaded nanoparticle. (B) Biodistribution profile of different formulations of Alexa-488-labeled cytC after intravenous injection into H460 xenograft mice. (C) Tumor growth inhibition of different formulations of cytC (40 μg/kg) or MPS−cytC (160 μg/kg) in an H460 xenograft mouse model. Figures combined and reproduced with permission from ref 115. Copyright 2012 Elsevier.

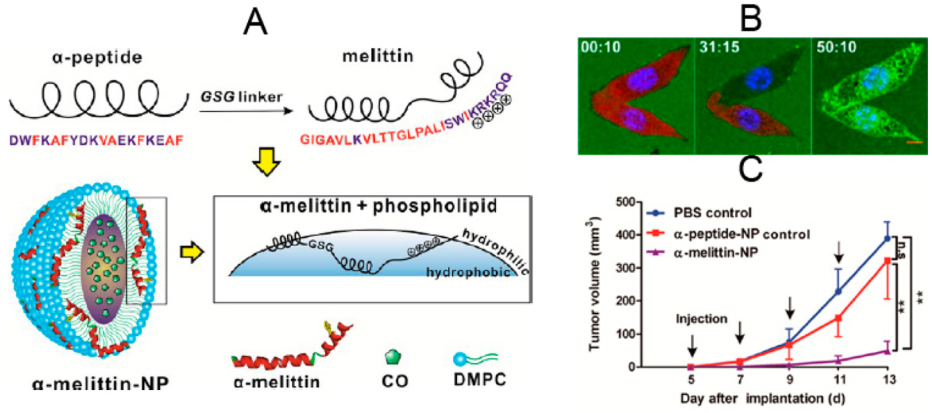

Figure 5. Efficient delivery of cytolytic peptide, melittin, to tumor cells using HDL. (A) Schematic of loading α-melittin to HDL nanoparticles (α-melittin-NP). (B) Real-time imaging of the release of FITC-α-melittin (green) from HDL nanoparticles attacking tumor cells expressing KatushkaS158A (red) with confocal microscopy. KatushkaS158A (red) inside the cells decreased over time, while FITC-α-melittin (green) increased inside the cells, indicating that FITC-R-melittin was released from the HDL nanoparticles and made pores on the cell membrane, which allowed KatushkaS158A to leak out of the cells. (C) Tumor growth inhibition of different formulations in a B16F10 tumor model. Figures combined and reproduced from ref 116. Copyright 2013 American Chemical Society.

and analyzed for quality control.[118] However, peptide/protein antigens alone often have poor immunogenicity;[188] therefore, co-administration of an adjuvant, such as TLR agonist, is needed.[189,190] Fischer *et al.* addressed this issue by coloading protein antigens and adjuvants in HDL to ensure their colocalized delivery to APCs.[118] Specifically, they prepared HDL containing nickel-modified lipids and recombinant apolipoprotein using the sodium cholate dialysis method. To load the recombinant viral and bacterial antigens into HDL, influenza hemagglutinin 5 (H5) and *Yersinia pestis* LcrV

DOI: 10.1021/acsnano.5b07522
ACS Nano 2016, 10, 3015−3041

proteins were modified with a polyhistidine group, enabling their efficient conjugation to nickel–lipid-containing HDL.[191,192] In addition, they also adsorbed either MPLA or CpG as an adjuvant into the same HDL nanoparticles by utilizing hydrophobic interaction between the adjuvants and HDL. These HDL nanoparticles with their size ranging 10–20 nm carried ~21 protein antigens and 3 ± 1 MPLA or 6 ± 1 CpG molecules per particle. Their *in vivo* study showed that antigen-conjugated HDL/MPLA (2.5 μg antigen/animal and 0.2 μg MPLA/animal) as well as antigen-conjugated HDL/CpG (2.5 μg antigen/animal and 2.2 μg CpG/animal) achieved 5–10 times higher antibody titers, compared with vaccination with the mixture of free antigen and adjuvant.

Delivery of Nucleic Acids. RNA interference (RNAi) is a promising gene therapy, due to its high specificity and potential to down-regulate selected proteins involved in the pathogenesis of different diseases.[193] However, there are several barriers to overcome before siRNA can be efficiently delivered to target cells and down-regulate target proteins. First, siRNA can be readily degraded by nucleases in serum;[194,195] thus, measures should be taken to protect siRNA from rapid degradation *in vivo*. Second, the RES system can rapidly clear foreign entities, preventing accumulation of siRNA at the desired target organs. Therefore, an ideal siRNA delivery system should shield siRNA from RES and permit accumulation and delivery of siRNA to the target cells.[196] Third, once internalized into target cells, siRNA can be degraded in endosomes/lysosomes. Thus, the delivery system should allow cytosolic delivery of cargo so that siRNA is recognized and associate with RNA-induced silencing complex (RISC) to degrade target mRNA.[197,198] Despite these hurdles, significant progress has been made over the past decade. For example, chemical modification[199] or encapsulation of siRNA into different carriers, such as liposomes,[200] polymers,[201] and nanoparticles,[202] can protect siRNA from degradation. Additionally, PEGylation of these carriers allows evasion of the RES and enhances circulation half-life *in vivo*,[203] while modification of these carriers with targeting ligands promotes selective targeting to target organs and cells. Finally, the use of moieties promoting endosome escape can further improve the gene silencing effect of siRNA.[204,205] Recent studies have shown that HDL is a promising delivery system for siRNA, as HDL can overcome the barriers mentioned above with mechanisms of action distinct from those of other conventional nanocarriers. Notably, endogenous HDL has been reported to be involved in the transport of microRNA *in vivo*,[206] suggesting the potential of using HDL as a natural delivery carrier for nucleic acids.

Modification of Nucleic Acids with Lipophilic Groups. Modification of siRNA with lipophilic groups, such as cholesterol, offers a convenient method of loading siRNA in HDL.[207] Soutschek *et al.* conjugated cholesterol to ApoB siRNA that was chemically stabilized with phosphorothioate backbone at the 3′ end of the sense and antisense strands and two 2′-O-methyl nucleotides at the 3′ end of the antisense strand.[207] ApoB siRNA conjugated with cholesterol (Cho-ApoB-siRNA) displayed increased stability in human serum than the unconjugated form. When Cho-ApoB-siRNA (50 mg/kg) was intravenously injected to C57BL/6 mice, a significant level of Cho-ApoB-siRNA was detected in the liver and jejunum, whereas little or no unconjugated ApoB siRNA was detected in these organs. Cho-ApoB-siRNA was better able to silence ApoB mRNA in the liver and jejunum, decrease plasma levels of ApoB protein, and reduce total cholesterol, compared with unconjugated ApoB-siRNAs.

Wolfrum *et al.* studied the mechanism by which siRNA conjugated to cholesterol and other lipophilic groups were delivered to their target organs and cells.[72] Since lipoproteins, such as HDL, LDL, and VLDL, play important roles in the transport of cholesterol,[208] the authors evaluated whether siRNA modified by various lipophilic groups, such as cholesterol and fatty acids with different chain lengths (C_{12}–C_{43}), could bind to lipoproteins and facilitate *in vivo* delivery of siRNA. The results indicated that siRNA conjugated to cholesterol or relatively long fatty acid chains bound to HDL particles, whereas siRNA conjugated to short or medium chain length fatty acids did not bind to lipoproteins but preferentially associated with serum albumin or remained in an unbound form. Cholesterol-ApoB siRNA preassembled in HDL was 8–15-fold more effective at silencing ApoB expression in the liver and jejunum, compared with administration of cholesterol-ApoB siRNA only. Using HDL labeled with ^{125}I-tyramine cellobiose (TC) and loaded with ^{32}P-cholesterol-siRNA, the authors found that the half-life of HDL was 4.8 days, whereas the half-life of HDL-bound cholesterol-siRNA was only about 1 h. Since the cholesterol-siRNA was stabilized by chemical modification through use of a phosphorothioate backbone and 2′-O-methyl nucleotides, the difference in half-life was not due to the faster degradation and clearance of cholesterol-siRNA in the plasma. The difference was rather due to selective uptake of cholesterol-siRNA from HDL through a mechanism independent of endocytosis of whole HDL particles. The uptake of HDL-bound cholesterol-siRNA was dependent on SR-BI expression on the target cells, as mice lacking SR-BI expression exhibited a 2-fold increase in half-life of HDL-bound cholesterol-siRNA, compared with the control wild-type mice.

Rather than using endogenous HDL purified from plasma to deliver cholesterol-siRNA, Nakayama *et al.* prepared HDL with recombinant apolipoprotein A1 (ApoA1) or apolipoprotein E3 (ApoE3) and phosphatidylcholine lipids for delivery of cholesterol-siRNA (chol-siRNA) to the liver.[119] When chol-siRNA was incubated with ApoA1-containing HDL (A-lip) or ApoE-containing HDL (E-lip) at ratios between 1:1 and 4:1, the incorporation efficiency of chol-siRNA was 90–95%. Forty-eight hours after intravenous injection of 50 mg/kg of chol-siApoB-1 complexed with A-lip, hepatic mRNA was inhibited by 40–60%, similar to that achieved by the complex of chol-siApoB-1 and purified mouse HDL (mHDL). In the same study, ApoE-containing HDL (E-lip) was found to be more effective than ApoA1-containing HDL (A-lip) at delivery of cholesterol-siRNA: over 80% reduction of hepatic ApoB mRNA was observed when 30 mg/kg chol-siApoB-1 or chol-siApoB-2 complexed with E-lip was intravenously injected in mice (Figure 6).

Yang *et al.* studied the intracellular delivery profile of cholesterol-modified siRNA using HDL prepared with lipids and ApoA1 mimetic peptides.[74,209] They modified bcl-2 siRNA with cholesterol (chol-si-bcl-2) and incubated it with preformed HDL at room temperature for 30 min, leading to successful insertion of chol-si-bcl-2 into the lipid layers of HDL. Chol-si-bcl-2-HDL had a size of 25.3 ± 1.2 nm and was stable in 10% fetal bovine serum (FBS) or 10% human plasma at 4 or 37 °C for 3 h. When FITC-chol-si-bcl-2-HDL was incubated with SR-BI high-expressing KB cells, more than 90% of the total intracellular FITC-chol-si-bcl-2 signal was in the cytosol, indicating direct cytosolic delivery of chol-siRNA. Western blot revealed

DOI: 10.1021/acsnano.5b07522
ACS Nano 2016, 10, 3015–3041

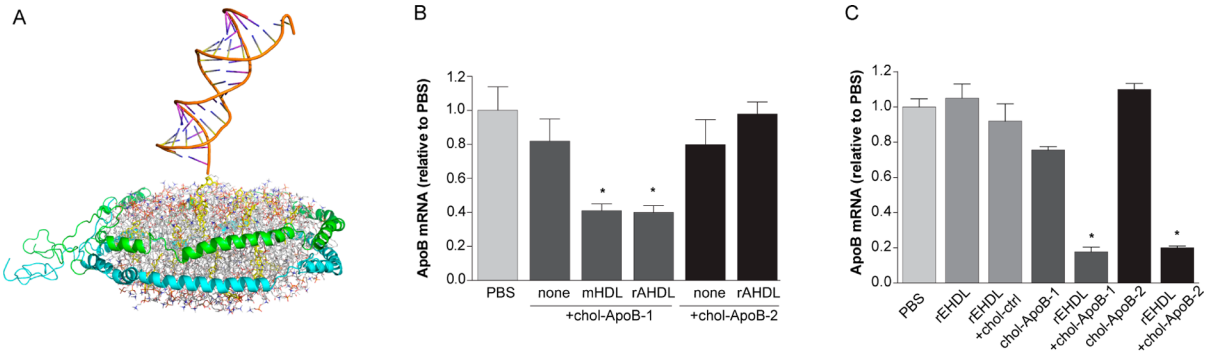

Figure 6. Efficient delivery of siRNA molecules to hepatocytes using HDL. (A) Schematic of incorporation of cholesterol modified siRNA (chol-siRNA) into an HDL nanoparticle. (B) *In vivo* ApoB mRNA silencing effect of A-lip-chol-siApoB-1 and A-lip-cholsiApoB-2 48 h after intravenous injection of 50 mg/kg siRNA to C57BL/6 mice. ApoB mRNA silencing with chol-siRNA alone and chol-siApoB complexed with purified mouse HDL were used as control groups. (C) *In vivo* ApoB mRNA silencing effect of E-lip-siApoB-1 and E-lip-siApoB-2 48 h after intravenous injection of 30 mg/kg siRNA to C57BL/6 mice. Data represent mean ± SD; *$P < 0.05$. Figures combined and reproduced with permission from ref 119. Copyright 2012 Nature Publishing Group.

that chol-si-bcl-2-HDL, at a dose of 400 nM, reduced Bcl-2 expression to 35 ± 9% of the untreated control, whereas an equivalent dose of chol-si-bcl-2 alone only reduced Bcl-2 expression to 84 ± 8% of the untreated control. In addition, chol-si-bcl-2-HDL was also more efficient at inducing apoptosis of tumor cells, compared with free chol-si-bcl-2.

HDL has also been used *in vivo* to deliver siRNA to tumor cells, the majority of which express SR-BI. Ding *et al.* modified siRNA for Pokemon gene with cholesterol (chol-siRNA), which was then complexed with lipids by the sodium cholate dialysis method.[210] The complex was then incubated with ApoA1 in solution to form HDL/chol-siRNA. At the optimal volume ratio, the loading efficiency of chol-siRNA into HDL was over 99%. The HDL/chol-siRNA exhibited improved stability in serum relative to chol-siRNA. Chol-siRNA in HDL was mostly intact at 12 h, while the naked chol-siRNA was degraded after 3 h. The release of chol-siRNA from HDL was very slow in PBS at 37 °C, with less than 1% of the cargo released within 24 h. HDL-incorporated chol-siRNA enhanced cytosolic delivery of siRNA, gene silencing, and cell killing, compared with naked chol-siRNA. In addition, Cy5-chol-siRNA in HDL accumulated more efficiently in the tumor regions of HepG2-tumor-bearing nude mice, compared with Cy5-chol-siRNA-loaded lipoplexes, as measured by optical imaging after systemic administration. Moreover, intravenous injection of HDL-incorporated chol-siRNA (25 mg of chol-siRNA-Pokemon/mouse) every 2 days with a total of eight injections was significantly more effective at inhibiting tumor growth and reducing Pokemon and Bcl-2 protein expression in comparison to free chol-siRNA.

In addition to delivery of siRNA to the above major target organs, HDL has also been used to deliver siRNA to other tissues/organs. For example, in one study, HDL was used to deliver cholesterol-conjugated siRNA for organic anion transporter 3 (chol-siOAT3) into brain capillary endothelial cells. The results showed that HDL-chol-siOAT3 significantly decreased OAT3 mRNA levels in BCECs after intravenous injection, while free chol-siOAT3 failed to achieve this.[121]

Complexation of Nucleic Acids with Polylysine. Although conjugation of lipophilic groups to siRNA is the most widely reported method of incorporating siRNA into HDL, there are other methods reported to produce siRNA-loaded HDL. Shahzad *et al.* utilized polylysine complexed with STAT3-siRNA in order to neutralize the negative charges of phosphate groups on siRNA. The authors successfully encapsulated the siRNA−polylysine complex into HDL, composed of lipids and ApoA1, with an encapsulation efficiency of over 90%.[120] STAT3-siRNA/HDL mediated over 80% knockdown of STAT3 in SKOV3 ovarian carcinoma cells *in vitro*. After a single intravenous injection of STAT3-siRNA/HDL (0.2 mg/kg siRNA) into SKOV3 ovarian carcinoma-bearing mice, STAT3 protein level was reduced by 88%. While injection of STAT3-siRNA/HDL alone showed some therapeutic effect in several different tumor models, enhanced effects were observed upon co-administration of chemotherapeutic drugs (Figure 7).

HDL for Imaging Studies. Unlike other nanocarriers, such as liposomes, micelles, and nanoparticles, HDL has the intrinsic ability to target atherosclerotic plaques as well as a broad range of tumor cells expressing SR-BI.[211] Recent studies have exploited this intrinsic targeting capability of HDL for various biomedical diagnostic applications, including imaging of atherosclerotic plaques and tumors.

Atherosclerotic Plaque Imaging Using HDL. Early diagnosis is crucial for effective therapeutic intervention against atherosclerosis, which is a major health problem across the world.[102] Magnetic resonance imaging (MRI) has been widely used for medical imaging. However, for atherosclerotic plaque imaging, the majority of conventional MRI contrast agents, such as gadolinium (Gd^{3+}) ions, are not able to reach the target sites efficiently. In order to improve the MRI signal in plaque regions, Frias *et al.* formulated a phospholipid-based MRI contrast agent into reconstituted HDL, which was prepared with ApoA1 protein and phospholipids using the sodium cholate dialysis method.[212] The resulting MRI contrast agent, Gd-DGPA-DMPE-loaded HDL, had diameter of approximately 9 nm and contained 15−20 molecules of Gd-DGPA-DMPE per HDL nanoparticle. One day after intravenous injection of HDL into ApoE-knockout mice with atherosclerosis, the contrast agent was predominantly localized at the atherosclerotic plaque. HDL labeled with green fluorescent phospholipids was used to visualize the distribution pattern of HDL in the atherosclerotic plaques at the cellular level. At 24 h post-intravenous injection, HDL was mainly found to be colocalized with CD68-positive macrophages in the intimal layer of the aorta.

In a separate study, Cormode *et al.* used ApoA1 mimetic peptide rather than ApoA1 protein to prepare HDL for atherosclerotic plaque imaging.[88] The lipid-based MRI contrast agent, Gd-DTPA-DMPE, and fluorescent lipid Rhod-PE were

DOI: 10.1021/acsnano.5b07522
ACS Nano 2016, 10, 3015−3041

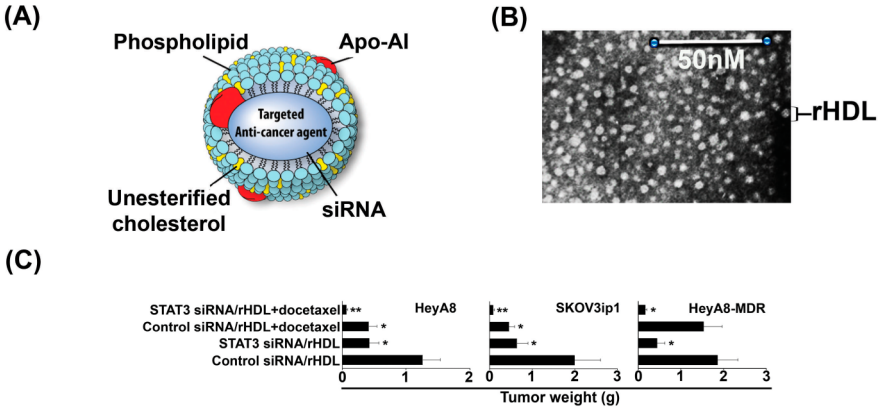

Figure 7. Efficient delivery of STAT3 siRNA molecules to tumor cells using HDL. (A) Schematic of encapsulation of siRNA into HDL after complexation with poly lysine. (B) TEM of siRNA-loaded HDL. (C) *In vivo* antitumor effect of STAT3 siRNA/rHDL in chemosensitive (HeyA8 and SKOV3ip1) and chemoresistant (HeyA8-MDR) mouse models of ovarian carcinoma. Figures combined and reproduced with permission from ref 120. Copyright 2011 Elsevier.

incorporated into HDL reconstituted with DMPC and ApoA1 mimetic peptide (37pA). The particle size averaged about 7.6 nm, as indicated by dynamic light scattering (DLS) measurements. In contrast, when Gd-DTPA-DMPE was incorporated into DMPC and fluorescent lipid Rhod-PE in the absence of ApoA1 mimetic peptide (37pA), the resulting particle size was about 15.0 nm, which was due to the formation of micelles rather than HDL. Quantitative analysis showed that the total number of lipids per HDL was 113, and the number of Gd-DTPA-DMPE was 42. When HDL and micelles were intravenously injected in atherosclerotic (ApoE-knockout) mice, MRI imaging clearly showed accumulation of HDL in the aorta. Moreover, HDL achieved a greater normalized enhancement ratio (% NER) of 94%, while the % NER achieved by micelles was only 16%. This clearly indicated that ApoA1 mimetic peptide (37pA) played an important role in enhancing the accumulation of MRI contrast agent in atherosclerotic plaques. By performing CLSM on sections of excised aorta and labeling macrophages with Alexa-647-CD68 (green), they confirmed that the fluorescent lipids delivered by HDL were localized in macrophages (Figure 8). These results are in line with previous results achieved using HDL reconstituted with lipids and ApoA1 proteins.

Several other tracers, such as near-infrared fluorescent dyes,[102,125] gold,[59] iron oxide,[213] and quantum dots,[58] have also been loaded into HDL reconstituted with phospholipids and ApoA1 proteins for imaging atherosclerotic plaques. This array of imaging agents formulated into HDL greatly expands the range of techniques that can be applied for atheroma imaging.

Tumor Imaging Using HDL. As mentioned above, HDL itself has great potential to accumulate in tumors, underscoring the potential utility of HDL for imaging and detection of tumors. Cao *et al.* synthesized a novel and chemically stable fluorescent dye (BchlBOA) with excitation at 752 nm and emission at 762 nm, suitable for deep tissue imaging due to its high absorbance coefficient and good fluorescence quantum yield in the near-infrared spectrum.[214] They incorporated BchlBOA into HDL reconstituted with DMPC, cholesterol oleate, and ApoA1. The dye-loaded HDL (HDL-BchlBOA) had a size of approximately 12 nm, similar to that of native HDL. When HDL-BchlBOA was incubated with cells either expressing SR-BI (SR-BI positive) or not expressing SR-BI (SR-BI negative), only SR-BI-positive cells exhibited significant uptake of HDL-BchlBOA, while SR-BI-negative cells had minimal uptake of HDL-BchlBOA. The uptake of HDL-BchlBOA by SR-BI-positive cells was inhibited in the presence of 25-fold excess native HDL, which is a natural ligand for the SR-BI receptor, indicating SR-BI receptor-mediated cellular internationalization. Moreover, when HDL-BchlBOA was intravenously injected into human epidermoid carcinoma KB tumor xenografts, the fluorescence signal was detected in the tumor and lasted for a minimum of 72 h.

In order to image the intracellular delivery profile of HDL cargoes, Zhang *et al.* used ApoA1 mimetic peptide rather than full-length ApoA1 to synthesize reconstituted HDL containing DMPC and cholesterol oleate.[73,215] In their study, fluorescent dye DiR-BOA was loaded into HDL as its cargo. For imaging purposes, HDL lipids or peptides were partially labeled with fluorescein. Similar to the uptake profile of HDL reconstituted with full-length proteins, cargoes of ApoA1 mimetic peptide HDL were efficiently taken up by SR-BI-positive cells but not by SR-BI-negative cells, and the uptake was inhibited in the presence of native HDL. Moreover, while HDL cargoes of DiR-BOA were detected in the cytosol, other components of HDL, such as fluorescein-labeled lipids and fluorescein-labeled peptides, were still on the plasma membrane, indicating that the cargo materials were taken up through a non-endocytic pathway. The subcellular fractionation assay showed that 63% of the fluorescent cargo was in the cytosol, while 12 and 25% were in the nuclei and other subcellular organelles, respectively. To investigate the efficacy of HDL-mediated targeting of SR-BI-expressing tumor cells *in vivo*, mice bearing human epidermoid carcinoma KB cells (SR-BI positive) on the left flank and HT1080 human fibrosarcoma cells (SR-BI negative) on the right flank were administered with HDL. The whole-body optical imaging showed that HDL preferentially accumulated in the SR-BI-positive tumor sites rather than the SR-BI-negative tumor sites, with 3.8-fold higher fluorescence intensity/gram of tumor tissue associated with the SR-BI-positive tumor sites (Figure 9).

Recently, the same HDL platform reconstituted with DMPC, cholesteryl oleate, and ApoA1 mimetic peptide has been used not only for primary tumor imaging but also for metastatic tumor imaging.[83] Specifically, HDL was loaded with porphyrin, whose fluorescence was highly silenced in intact HDL. However, upon arrival at tumor regions and internalization by tumor cells, the monomeric porphyrin molecules were released from

DOI: 10.1021/acsnano.5b07522
ACS Nano 2016, 10, 3015−3041

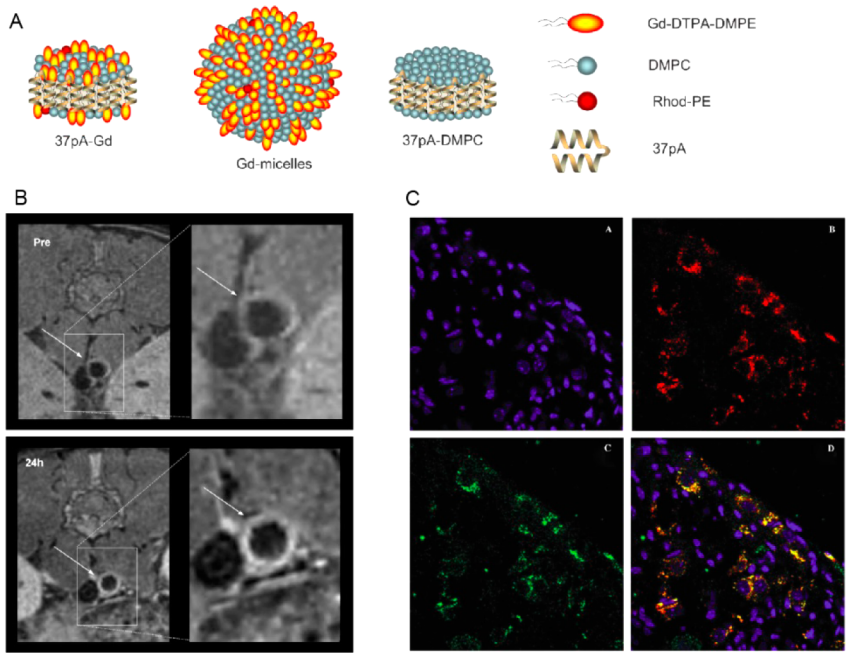

Figure 8. Use of HDL to deliver a MRI contrast agent for atherosclerotic plaque imaging. (A) Schematic of Gd-loaded HDL (37pA-Gd), Gd-loaded micelles (Gd-micelles), and blank HDL (37pA-Gd). (B) MRI images of the aorta of an ApoE-KO mouse. Top panel: images acquired before injection of 37pA-Gd. Bottom panel: images acquired 24 h after injection of 37pA-Gd. The images on the right of each panel are enlargements of the white box area, where the aorta is indicated by the white arrow. (C) Confocal microscopy images of aortic tissue from an ApoE-KO mouse intravenously injected with 37pA-Gd 24 h prior to excision. Blue: nuclei stained by DAPI. Red: Rhodamine lipid in HDL. Green: macrophages labeled by Alexa-647-labeled CD68 antibody. The yellow color in the merged images indicates that the HDL is colocalized with the macrophages. Figures combined and reproduced with permission from ref 88. Copyright 2008 Wiley.

HDL and became highly fluorescent. Such an activatable mechanism allows HDL to image both primary and metastatic tumors with very low background. The intrinsic metal chelation property of porphyrin also enabled HDL to be easily labeled with ^{64}Cu for PET (positron emission tomography) imaging, which could provide useful information on biodistribution. Moreover, the phothodynamic reactivity of released porphyrin could be utilized for selective photodynamic therapy. These results clearly show that the application of HDL can be expanded and customized by choosing proper imaging agents as HDL cargo.

In addition to utilizing HDL's intrinsic interaction with SR-BI for tumor imaging, different targeting ligands, such as RGD, folate, and EGF have been attached to HDL,[148] thus potentially expanding the spectrum of cancer types that can be targeted by HDL-based strategies while reducing the off-target effects on noncancerous cells.

CONCLUSION AND FUTURE PERSPECTIVE

Synthetic HDL nanoparticles are close mimics of abundant natural lipoprotein and thus are safe when given at large doses. The results of clinical trials and formal toxicology studies have indicated that sHDL nanoparticles appear to be better tolerated than inorganic and polymer nanoparticles. Indeed, sHDLs have been clinically administered at doses tens to hundreds times higher than inorganic nanoparticles of similar sizes. Such differences are likely due to the way nanoparticles are recognized by the body and eliminated. The net particle charge, density, fluidity at body temperature, and ability to interact with blood components are distinctly different for synthetic lipoproteins, inorganic and polymer-based nanoparticles. However, loading of small molecules or imaging agents into HDL, decoration of HDL's surface with peptide antigens and targeting ligands, and incorporation of nucleotides could all affect the charge, density, and stability in plasma. Further evaluations are needed to understand which modifications are benign or detrimental to sHDL's safety profiles.

Because of the stealth properties of sHDL mimicking the natural HDL carrier, sHDL has been reported to circulate for an extended period of time. Other nanoparticles require surface modification by PEG to prolong their circulation half-life. While PEG is used widely, it has been reported that PEGylated drug products can elicit immunologic responses characterized by PEG-neutralizing antibodies that can reduce circulation time of PEGylated products after repeated injections and potentially cause serious adverse reactions. Therefore, the extended circulation time of sHDL without the need for PEGylation is an attractive property. However, drug loading in sHDL can alter their circulation time, and covalent binding of drugs or macromolecules on the surfaces of sHDL could inadvertently induce immune responses and alter their pharmacokinetics. Therefore, the effect of drug loading and incorporation on pharmacokinetics of drug–sHDL formulations requires further investigation.

Another critical process for circulation time and targeting ability of sHDL particles is their dynamic remodeling in plasma. Once HDL nanoparticles are infused, they can exchange their proteins, lipids, and cargo with endogenous plasma lipoproteins.[216] Other nanoparticle products also undergo remodeling, as lipoprotein corona forms on inorganic nanoparticles in plasma.[217] When non-PEGylated liposomes, such as Visudyne, are administered, they are rapidly remodeled, and the drug originally loaded in liposomes is found in HDL fraction within minutes.[218] The administered dose of sHDL is typically several-fold higher than the levels of endogenous lipoproteins; thus, the

DOI: 10.1021/acsnano.5b07522
ACS Nano 2016, 10, 3015–3041

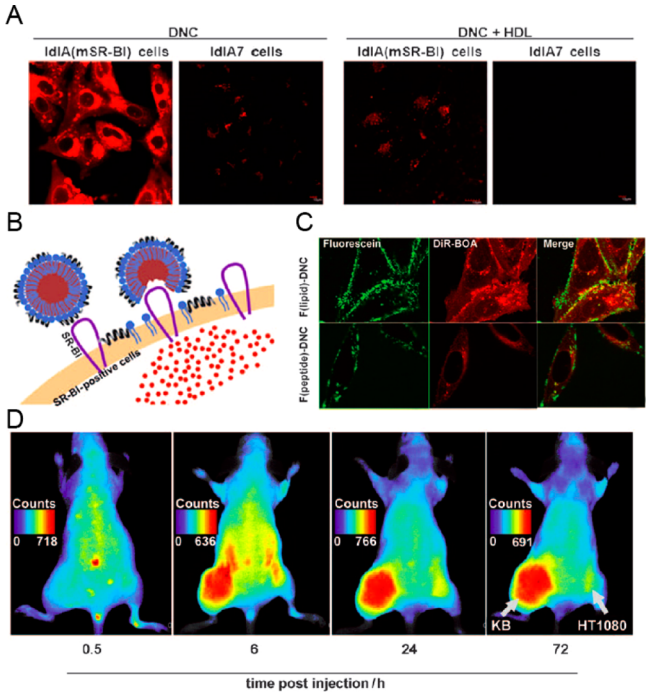

Figure 9. Use of HDL to deliver a near-infrared fluorescent dye for tumor imaging. (A) Confocal microscopy imaging of uptake of DiR-BOA-loaded HDL (DNC) by ldlA transfected with SR-BI [ldl(mSR-BI)] or not transfected with SR-BI (ldlA7) in the absence of excess HDL (left panel) and in the presence of excess HDL (right panel). (B) Schematic depiction of the uptake of HDL cargoes *via* the SR-BI-mediated pathway. (C) Confocal microscopy images of ldlA (mSR-BI) (SR-BI+) cells showing the fluorescein-labeled lipid (green color in top panel) and peptide (green color in bottom panel) localized on the cell surface and the DiR-BOA cargo (red) in the cytosol. (D) Optical imaging of the tumor targeting of DiR-BOA-loaded HDL in tumor-bearing mice using the whole-body optical imaging system. Figures combined and reproduced with permission from ref 73. Copyright 2009 Wiley.

infused sHDL dominates the composition of lipoproteins. Both the rate and extent of lipoprotein remodeling depend on sHDL protein−lipid binding affinity and fluidity of the sHDL lipid membrane, along with multiple other factors. Therefore, it is critical to develop experimental tools and reagents to further understand the process of lipoprotein remodeling *in vitro* and *in vivo* and to incorporate the knowledge gained from these fundamental studies into the selection process of sHDL delivery nanomedicines for clinical translation.

Unlike other conventional nanoparticles, sHDL intrinsically targets several different organs/tissues, including atherosclerotic plaques, hepatocytes, and SR-BI-positive tumor cells. The targeting of sHDL could be further augmented by incorporating targeting ligands. While dye-loaded sHDL are found in atheroma and SR-BI-positive tumors,[73,102] the extent of drug enrichment at the target tissue that HDL nanoparticle delivery offers over that of naked drug administration remains unclear. Another critical unanswered question is whether sHDL is capable of crossing the blood brain barrier. While it is believed that HDL is capable of crossing the BBB, the question remains whether it is solely the protein component or the entire HDL nanoparticle that can cross the BBB.[219] Intrinsic tissue targeting by HDL, incorporation of targeting moieties, and the effect of plasma remodeling on passive and active targeting represent the frontier of sHDL research that will enhance our understanding of interactions between nanomaterials and biological systems while extending our arsenal of nano delivery carriers suitable for clinical translation.

We have pointed that the cGMP manufacturing processes have been successfully established for multiple sHDL products; however, for drug-loaded sHDLs, their scalability of manufacturing, cost, yields, and purities are yet to be determined. While most HDLs used for atherosclerosis treatment are made of full-length proteins (*e.g.*, ApoA1, ApoA1Milano, and proApoA1), their utility as drug delivery vehicles is limited because the proteins are either purified from human plasma or produced by recombinant technology using expensive multistep processes. In this regard, application of ApoA1 mimic peptides for HDL-mediated drug delivery holds significant promise; sHDL composed of peptides are inexpensive, produced by a well-controlled chemical synthesis, and lack toxic or immunogenic impurities such as viruses, endotoxin, host cell proteins, or protein aggregates. However, the majority of drug-loaded sHDLs currently require purification to narrow the size distribution and remove non-encapsulated drug. It would be critical to define the process for spontaneous assembly of ApoA1 peptide, phospholipid, and drug into drug−sHDL formulations without the need for subsequent purification as this would expedite the cGMP manufacturing process and clinical translation.

Several types of molecules have been successfully incorporated into sHDL delivery nanoparticles, including small-molecule drugs, dyes, siRNA, peptides, and proteins. The small size of HDL (8−12 nm) and its well-defined nanodisk structure leave limited space for drug incorporation. Many lipophilic drugs have been incorporated into the core of sHDL *via* physical partitioning. Hydrophilic drugs require modification with lipophilic moieties prior to sHDL incorporation.[72] Oligonucleotides were modified with cholesterol and fatty acid moieties in order to incorporate into sHDL's lipid bilayer either by partitioning or by binding to polylysine to neutralize their charge prior incorporation.[72,120] Peptide- and protein-based therapeutics have been either inserted into the lipid membrane *via* a transmembrane domain or covalently attached to lipid or protein components of sHDL. The incorporation of drugs into sHDL often alters the size, shape, and surface properties. In fact, many drug-loaded sHDLs are spherical and 20−30 nm in size, resembling LDL particles.[84] Drug loading varies between different systems, ranging from 1 to 3 drug molecules per HDL particle to up to 10% of total particle mass. Significant changes in such physicochemical properties of sHDL may alter its stealth properties. As the size of HDL is similar to the size of an antibody, HDL-based delivery could be compared with antibody−drug conjugates (ADC). Recent findings in the ADC field suggest an optimal loading of 2−4 molecules to elicit a therapeutic effect without altering antibody pharmacokinetics.[220] Application of a similar concept to HDL delivery will likely be beneficial.

Synthetic HDL nanoparticles themselves are potent therapeutic agents. Apart from their known ability to treat atherosclerosis by removing excess cholesterol in hardened arteries, HDL has anticancer activity by cellular cholesterol depletion,[221,222] activity in sepsis by lipopolysaccharide neutralization,[221] and ability to alter Alzheimer's disease pathology by amyloid peptide removal and other diseases.[223,224] In most pharmacology studies, when beneficial effects are seen from drug−HDL formulations, the benefit is attributed to the sHDL's ability to deliver drug to target tissue(s). However,

DOI: 10.1021/acsnano.5b07522
ACS Nano 2016, 10, 3015−3041

examination of relative contributions of sHDL tissue targeting *versus* synergetic effect of drug and sHDL is important in nanomedicine design. The composition of sHDL (lipid type, particle size, charge, *etc.*) affects sHDL's pharmacology and ability to incorporate drugs and may be differentially optimized to exploit synergetic *versus* drug targeting delivery effects.[56,223]

Overall, it remains to be seen how the exciting progress made in the field of HDL-based therapy can evolve to reprogram HDL as a platform technology for nanomedicines. Clinical translation of HDL-based therapeutics may offer innovative solutions to treat and diagnose various human pathologies.

AUTHOR INFORMATION

Corresponding Authors

*E-mail: moonjj@umich.edu.
*E-mail: annaschw@umich.edu.

Notes

The authors declare no competing financial interest.

ACKNOWLEDGMENTS

This work is supported in part by Broomfield International Student Fellowship (R.K.), AHA predoctoral fellowship (15PRE25090050, R.K.), NIH (UL1TR000433, J.J.M.), the John S. and Suzanne C. Munn Cancer Fund of the UM Comprehensive Cancer Center (J.J.M.), Melanoma Research Alliance (J.J.M.), NSF CAREER Award (J.J.M.), an AHA scientist development grant (AHA 13SDG17230049, A.S.), UM 2014 MTRAC for Life Sciences (A.S.), an Upjohn research award from the UM College of Pharmacy (A.S.), NIH (R01GM113832, R21NS091555, A.S.), and Mcubed grant (J.J.M. and A.S.).

VOCABULARY

Lipoproteins, endogenous nanoparticles composed of apolipoproteins and lipids, classified by their densities into high-density (HDL), low-density (LDL), and very low density (VLDL), varying in size (8−80 nm), shape, protein−lipid composition, and physiological functions; **Apolipoproteins**, proteins that can associate with lipids, with six major apolipoprotiens including ApoA, ApoB, ApoC, ApoD, ApoE, and ApoH; **Reconstituted HDL (rHDL) or synthetic HDL (sHDL)**, lipoprotein nanoparticles assembled from full-length apolipoprotein or synthetic apolipoprotein mimetic peptide; **Apolipoprotein mimetic peptides**, short 17−40 amino acid long synthetic peptides designed to bind lipids, form lipoprotein, and perform apolipoprotein-like functions; **Multifunctional nanoparticles**, nanoparticles that have multiple functions including tissue targeting, delivery of therapeutics (small molecules, peptides/proteins, nucleic acids) to various target cells, and imaging of human pathologies for diagnostic purposes

REFERENCES

(1) Kingwell, B. A.; Chapman, M. J.; Kontush, A.; Miller, N. E. HDL-Targeted Therapies: Progress, Failures and Future. *Nat. Rev. Drug Discovery* **2014**, *13*, 445−64.

(2) Barr, D. P.; Russ, E. M.; Eder, H. A. Protein-Lipid Relationships in Human Plasma. II. In Atherosclerosis and Related Conditions. *Am. J. Med.* **1951**, *11*, 480−93.

(3) Gofman, J. W. Serum Lipoproteins and The Evaluation of Atherosclerosis. *Ann. N. Y. Acad. Sci.* **1956**, *64*, 590−5.

(4) Wang, M.; Briggs, M. R. HDL: The Metabolism, Function, and Therapeutic Importance. *Chem. Rev.* **2004**, *104*, 119−37.

(5) Movva, R.; Rader, D. J. Laboratory Assessment of HDL Heterogeneity and Function. *Clin. Chem.* **2008**, *54*, 788−800.

(6) Damiano, M. G.; Mutharasan, R. K.; Tripathy, S.; McMahon, K. M.; Thaxton, C. S. Templated High Density Lipoprotein Nanoparticles as Potential Therapies and for Molecular Delivery. *Adv. Drug Delivery Rev.* **2013**, *65*, 649−62.

(7) Nofer, J. R.; Kehrel, B.; Fobker, M.; Levkau, B.; Assmann, G.; von Eckardstein, A. HDL and Arteriosclerosis: Beyond Reverse Cholesterol Transport. *Atherosclerosis* **2002**, *161*, 1−16.

(8) Vance, D. E.; Vance, J. E. *Biochemistry of Lipids, Lipoproteins and Membranes*, 5th ed.; Elsevier B.V., 2008.

(9) Kontush, A.; Chapman, M. J. Antiatherogenic Function of HDL Particle Subpopulations: Focus on Antioxidative Activities. *Curr. Opin. Lipidol.* **2010**, *21*, 312−8.

(10) Vickers, K. C.; Palmisano, B. T.; Shoucri, B. M.; Shamburek, R. D.; Remaley, A. T. MicroRNAs are Transported in Plasma and Delivered to Recipient Cells by High-Density Lipoproteins. *Nat. Cell Biol.* **2011**, *13*, 423−33.

(11) Khan, M. L. N.; Drake, S. L.; Crockatt, J. G.; Dasseux, J. L. H. Single-Dose Intravenous Infusion of ETC-642, a 22-mer ApoA-I Analogue and Phospholipids Complex, Elevates HDL-C in Atherosclerosis Patients. *Circulation* **2003**, *108*, 563−564.

(12) Navab, M.; Anantharamaiah, G. M.; Reddy, S. T.; Van Lenten, B. J.; Datta, G.; Garber, D.; Fogelman, A. M. Human Apolipoprotein A-I and A-I Mimetic Peptides: Potential for Atherosclerosis Reversal. *Curr. Opin. Lipidol.* **2004**, *15*, 645−9.

(13) Navab, M.; Reddy, S. T.; Van Lenten, B. J.; Fogelman, A. M. HDL and Cardiovascular Disease: Atherogenic and Atheroprotective Mechanisms. *Nat. Rev. Cardiol.* **2011**, *8*, 222−32.

(14) Tuteja, S.; Rader, D. J. High-Density Lipoproteins in the Prevention of Cardiovascular Disease: Changing the Paradigm. *Clin. Pharmacol. Ther.* **2014**, *96*, 48−56.

(15) Cho, W. S.; Cho, M. J.; Jeong, J.; Choi, M.; Cho, H. Y.; Han, B. S.; Kim, S. H.; Kim, H. O.; Lim, Y. T.; Chung, B. H.; Jeong, J. Acute Toxicity and Pharmacokinetics of 13 nm-Sized PEG-Coated Gold Nanoparticles. *Toxicol. Appl. Pharmacol.* **2009**, *236*, 16−24.

(16) Khlebtsov, N.; Dykman, L. Biodistribution and Toxicity of Engineered Gold Nanoparticles: A Review of *in Vitro* and *in Vivo* Studies. *Chem. Soc. Rev.* **2011**, *40*, 1647−1671.

(17) Krause, B. R.; Remaley, A. T. Reconstituted HDL for the Acute Treatment of Acute Coronary Syndrome. *Curr. Opin. Lipidol.* **2013**, *24*, 480−6.

(18) Nanjee, M. N.; Doran, J. E.; Lerch, P. G.; Miller, N. E. Acute Effects of Intravenous Infusion of ApoA1/Phosphatidylcholine Discs on Plasma Lipoproteins in Humans. *Arterioscler., Thromb., Vasc. Biol.* **1999**, *19*, 979−89.

(19) Lerch, P. G.; Fortsch, V.; Hodler, G.; Bolli, R. Production and Characterization of a Reconstituted High Density Lipoprotein for Therapeutic Applications. *Vox Sang.* **1996**, *71*, 155−64.

(20) Spieker, L. E.; Sudano, I.; Hurlimann, D.; Lerch, P. G.; Lang, M. G.; Binggeli, C.; Corti, R.; Ruschitzka, F.; Luscher, T. F.; Noll, G. High-Density Lipoprotein Restores Endothelial Function in Hypercholesterolemic Men. *Circulation* **2002**, *105*, 1399−402.

(21) Bisoendial, R. J.; Hovingh, G. K.; Levels, J. H.; Lerch, P. G.; Andresen, I.; Hayden, M. R.; Kastelein, J. J.; Stroes, E. S. Restoration of Endothelial Function by Increasing High-Density Lipoprotein in Subjects with Isolated Low High-Density Lipoprotein. *Circulation* **2003**, *107*, 2944−8.

(22) van Oostrom, O.; Nieuwdorp, M.; Westerweel, P. E.; Hoefer, I. E.; Basser, R.; Stroes, E. S.; Verhaar, M. C. Reconstituted HDL Increases Circulating Endothelial Progenitor Cells in Patients with Type 2 Diabetes. *Arterioscler., Thromb., Vasc. Biol.* **2007**, *27*, 1864−5.

(23) Shaw, J. A.; Bobik, A.; Murphy, A.; Kanellakis, P.; Blombery, P.; Mukhamedova, N.; Woollard, K.; Lyon, S.; Sviridov, D.; Dart, A. M. Infusion of Reconstituted High-Density Lipoprotein Leads to Acute Changes in Human Atherosclerotic Plaque. *Circ. Res.* **2008**, *103*, 1084−91.

(24) Patel, S.; Drew, B. G.; Nakhla, S.; Duffy, S. J.; Murphy, A. J.; Barter, P. J.; Rye, K. A.; Chin-Dusting, J.; Hoang, A.; Sviridov, D.;

DOI: 10.1021/acsnano.5b07522
ACS Nano 2016, 10, 3015−3041

Celermajer, D. S.; Kingwell, B. A. Reconstituted High-Density Lipoprotein Increases Plasma High-Density Lipoprotein Anti-Inflammatory Properties and Cholesterol Efflux Capacity in Patients with Type 2 Diabetes. *J. Am. Coll. Cardiol.* **2009**, *53*, 962−71.
(25) Calkin, A. C.; Drew, B. G.; Ono, A.; Duffy, S. J.; Gordon, M. V.; Schoenwaelder, S. M.; Sviridov, D.; Cooper, M. E.; Kingwell, B. A.; Jackson, S. P. Reconstituted High-Density Lipoprotein Attenuates Platelet Function in Individuals with Type 2 Diabetes Mellitus by Promoting Cholesterol Efflux. *Circulation* **2009**, *120*, 2095−104.
(26) Tardif, J. C.; Gregoire, J.; L'Allier, P. L.; Ibrahim, R.; Lesperance, J.; Heinonen, T. M.; Kouz, S.; Berry, C.; Basser, R.; Lavoie, M. A.; Guertin, M. C.; Rodes-Cabau, J. ects of Reconstituted High-Density Lipoprotein Infusions on Coronary Atherosclerosis: a Randomized Controlled Trial. *JAMA* **2007**, *297*, 1675−82.
(27) Gille, A.; Easton, R.; D'Andrea, D.; Wright, S. D.; Shear, C. L. CSL112 Enhances Biomarkers of Reverse Cholesterol Transport After Single and Multiple Infusions in Healthy Subjects. *Arterioscler., Thromb., Vasc. Biol.* **2014**, *34*, 2106−14.
(28) Easton, R.; Gille, A.; D'Andrea, D.; Davis, R.; Wright, S. D.; Shear, C. A Multiple Ascending Dose Study of CSL112, an Infused Formulation of ApoA-I. *J. Clin. Pharmacol.* **2014**, *54*, 301−10.
(29) A Multiple Ascending Dose Study of CSL112 in Healthy Volunteers. https://clinicaltrials.gov/ct2/show/NCT01281774?term=CSL112&rank=3.
(30) A Single Ascending Dose Study Examining The Safety and Pharmacokinetic Profile of Reconstituted High Density Lipoprotein (CSL112) Administered to Patients. https://clinicaltrials.gov/ct2/show/NCT01499420?term=CSL112&rank=5.
(31) A Phase 2b Study of CSL112 in Subjects with Acute Myocardial Infarction. https://clinicaltrials.gov/ct2/show/NCT02108262?term=CSL-112&rank=1.
(32) Carlson, L. A. Effect of a Single Infusion of Recombinant Human Proapolipoprotein a-I Liposomes (Synthetic HDL) on Plasma-Lipoproteins in Patients with Low High-Density-Lipoprotein Cholesterol. *Nutr. Metab. Cardiovasc. Dis.* **1995**, *5*, 85−91.
(33) Eriksson, M.; Carlson, L. A.; Miettinen, T. A.; Angelin, B. Stimulation of Fecal Steroid Excretion After Infusion of Recombinant Proapolipoprotein A-I - Potential Reverse Cholesterol Transport in Humans. *Circulation* **1999**, *100*, 594−598.
(34) Bisgaier, C. L.; Rodriguez, W. V.; Lalwani, N. D.; Hartman, D.; Johansson, J. Pharmaceutical Formulations, Methods and Dosing Regimens for the Treatment and Prevention of Acute Coronary Syndromes. Patent Appl. CA2542726 C, 2012.
(35) Nissen, S. E.; Tsunoda, T.; Tuzcu, E. M.; Schoenhagen, P.; Cooper, C. J.; Yasin, M.; Eaton, G. M.; Lauer, M. A.; Sheldon, W. S.; Grines, C. L.; Halpern, S.; Crowe, T.; Blankenship, J. C.; Kerensky, R. Effect of Recombinant ApoA-I Milano on Coronary Atherosclerosis in Patients with Acute Coronary Syndromes: a Randomized Controlled Trial. *JAMA* **2003**, *290*, 2292−300.
(36) Dasseux, J.-L.; Oniciu, D. C.; Ackermann, R. Lipoprotein Complexes and Manufacturing and Uses Thereof. Patent Appl. US 20120232005 A1, 2012.
(37) Keyserling, C. H.; Hunt, T. L.; Klepp, H. M.; Scott, R. A.; Barbaras, R.; Schwendeman, A.; Lalwani, N.; Dasseux, J. L. CER-001, a Synthetic HDL-Mimetic, Safely Mobilizes Cholesterol in Healthy Dyslipidemic Volunteers. *Circulation* **2011**, 124.
(38) Tardif, J. C.; Ballantyne, C. M.; Barter, P.; Dasseux, J. L.; Fayad, Z. A.; Guertin, M. C.; Kastelein, J. J. P.; Keyserling, C.; Klepp, H.; Koenig, W.; L'Allier, P. L.; Lesperance, J.; Luscher, T. F.; Paolini, J. F.; Tawakol, A.; Waters, D. D. Effects of the High-Density Lipoprotein Mimetic Agent CER-001 on Coronary Atherosclerosis in Patients with Acute Coronary Syndromes: a Randomized Trial. *Eur. Heart J.* **2014**, *35*, 3277−3286.
(39) Hovingh, G. K.; Smits, L. P.; Stefanutti, C.; Soran, H.; Kwok, S.; de Graaf, J.; Gaudet, D.; Keyserling, C. H.; Klepp, H.; Frick, J.; Paolini, J. F.; Dasseux, J. L.; Kastelein, J. J. P.; Stroes, E. S. The Effect of an Apolipoprotein A-I-Containing High-Density Lipoprotein-Mimetic Particle (CER-001) on Carotid Artery Wall Thickness in Patients with Homozygous Familial Hypercholesterolemia: The Modifying Orphan Disease Evaluation (MODE) Study. *Am. Heart J.* **2015**, *169*, 736−U196.
(40) Effect of CER-001 on Plaque Volume in Homozygous Familial Hypercholesterolemia (HoFH) Subjects (MODE). https://clinicaltrials.gov/ct2/show/NCT01412034?term=CER001&rank=1.
(41) Exploratory Study of Plaque Regression (EXPRESS). https://clinicaltrials.gov/ct2/show/NCT01515241?term=CER001&rank=3.
(42) Di Bartolo, B. A.; Nicholls, S. J.; Bao, S.; Rye, K. A.; Heather, A. K.; Barter, P. J.; Bursill, C. The Apolipoprotein A-I Mimetic Peptide ETC-642 Exhibits Anti-Inflammatory Properties That Are Comparable to High Density Lipoproteins. *Atherosclerosis* **2011**, *217*, 395−400.
(43) Miles, J.; Khan, M.; Painchaud, C.; Lalwani, N.; Drake, S.; Dasseux, J. L. Single-Dose Tolerability, Pharmacokinetics, and Cholesterol Mobilization in HDL-C Fraction Following Intravenous Administration of ETC-642, a 22-mer ApoA-I Analogue and Phospholipids Complex, in Atherosclerosis Patients. *Proc. Arterioscl. Thromb. Vasc. Biol.* **2004**, *24*, E19−E19.
(44) Esperion Begins Multiple-Dose Study of ETC-642 (RLT Peptide) In Patients with Stable Atherosclerosis. http://www.prnewswire.com/news-releases/esperion-begins-multiple-dose-study-of-etc-642-rlt-peptide-in-patients-with-stable-atherosclerosis-71438847.html.
(45) Moguilevsky, N.; Varsalona, F.; Guillaume, J. P.; Gilles, P.; Bollen, A.; Roobol, K. Production of Authentic Human Proapolipoprotein-a-I in Escherichia-Coli - Strategies for the Removal of the Amino-Terminal Methionine. *J. Biotechnol.* **1993**, *27*, 159−172.
(46) Kempen, H. J.; Schranz, D. B.; Asztalos, B. F.; Otvos, J.; Jeyarajah, E.; Drazul-Schrader, D.; Collins, H. L.; Adelman, S. J.; Wijngaard, P. L. Incubation of MDCO-216 (ApoA-IMilano/POPC) with Human Serum Potentiates ABCA1-Mediated Cholesterol Efflux Capacity, Generates New Prebeta-1 HDL, and Causes an Increase in HDL Size. *J. Lipids* **2014**, *2014*, 923903.
(47) Davidson, W.; Silva, R.; Chantepie, S.; Lagor, W.; Chapman, M.; Kontush, A. Proteomic Analysis of Defined Hdl Subpopulations Reveals Particle-Specific Protein Clusters: Relevance to Antioxidative Function. *Arterioscler., Thromb., Vasc. Biol.* **2009**, *29*, 870.
(48) Bricarello, D. A.; Smilowitz, J. T.; Zivkovic, A. M.; German, J. B.; Parikh, A. N. Reconstituted Lipoprotein: A Versatile Class of Biologically-Inspired Nanostructures. *ACS Nano* **2011**, *5*, 42−57.
(49) Park, W.; Na, K. Advances in the Synthesis and Application of Nanoparticles for Drug Delivery. *Wiley Interdiscip. Rev. Nanomed. Nanobiotechnol.* **2015**, *7*, 494−508.
(50) El-Sayed, I. H.; Huang, X. H.; El-Sayed, M. A. Selective Laser Photo-Thermal Therapy of Epithelial Carcinoma Using Anti-EGFR Antibody Conjugated Gold Nanoparticles. *Cancer Lett.* **2006**, *239*, 129−135.
(51) Tkachenko, A. G.; Xie, H.; Coleman, D.; Glomm, W.; Ryan, J.; Anderson, M. F.; Franzen, S.; Feldheim, D. L. Multifunctional Gold Nanoparticle-Peptide Complexes for Nuclear Targeting. *J. Am. Chem. Soc.* **2003**, *125*, 4700−4701.
(52) Giljohann, D. A.; Seferos, D. S.; Prigodich, A. E.; Patel, P. C.; Mirkin, C. A. Gene Regulation with Polyvalent siRNA-Nanoparticle Conjugates. *J. Am. Chem. Soc.* **2009**, *131*, 2072.
(53) Wang, F.; Wang, Y. C.; Dou, S.; Xiong, M. H.; Sun, T. M.; Wang, J. Doxorubicin-Tethered Responsive Gold Nanoparticles Facilitate Intracellular Drug Delivery for Overcoming Multidrug Resistance in Cancer Cells. *ACS Nano* **2011**, *5*, 3679−3692.
(54) Rader, D. J. Molecular Regulation of HDL Metabolism and Function: Implications for Novel Therapies. *J. Clin. Invest.* **2006**, *116*, 3090−3100.
(55) Tall, A. R.; Yvan-Charvet, L.; Terasaka, N.; Pagler, T.; Wang, N. HDL, ABC Transporters, and Cholesterol Efflux: Implications for the Treatment of Atherosclerosis. *Cell Metab.* **2008**, *7*, 365−375.
(56) Schwendeman, A.; Sviridov, D. O.; Yuan, W. M.; Guo, Y. H.; Morin, E. E.; Yuan, Y.; Stonik, J.; Freeman, L.; Ossoli, A.; Thacker, S.; Killion, S.; Pryor, M.; Chen, Y. E.; Turner, S.; Remaley, A. T. The Effect of Phospholipid Composition of Reconstituted HDL on Its Cholesterol Efflux and Anti-Inflammatory Properties. *J. Lipid Res.* **2015**, *56*, 1727−1737.

DOI: 10.1021/acsnano.5b07522
ACS Nano 2016, 10, 3015−3041

(57) Thaxton, C. S.; Daniel, W. L.; Giljohann, D. A.; Thomas, A. D.; Mirkin, C. A. Templated Spherical High Density Lipoprotein Nanoparticles. *J. Am. Chem. Soc.* **2009**, *131*, 1384.
(58) Cormode, D. P.; Skajaa, T.; van Schooneveld, M. M.; Koole, R.; Jarzyna, P.; Lobatto, M. E.; Calcagno, C.; Barazza, A.; Gordon, R. E.; Zanzonico, P.; Fisher, E. A.; Fayad, Z. A.; Mulder, W. J. M. Nanocrystal Core High-Density Lipoproteins: A Multimodality Contrast Agent Platform. *Nano Lett.* **2008**, *8*, 3715−3723.
(59) Luthi, A. J.; Zhang, H.; Kim, D.; Giljohann, D. A.; Mirkin, C. A.; Thaxton, C. S. Tailoring of Biomimetic High-Density Lipoprotein Nanostructures Changes Cholesterol Binding and Efflux. *ACS Nano* **2012**, *6*, 276−285.
(60) McMahon, K. M.; Mutharasan, R. K.; Tripathy, S.; Veliceasa, D.; Bobeica, M.; Shumaker, D. K.; Luthi, A. J.; Helfand, B. T.; Ardehali, H.; Mirkin, C. A.; Volpert, O.; Thaxton, C. S. Biomimetic High Density Lipoprotein Nanoparticles For Nucleic Acid Delivery. *Nano Lett.* **2011**, *11*, 1208−1214.
(61) Xie, J.; Xu, C.; Kohler, N.; Hou, Y.; Sun, S. Controlled PEGylation of Monodisperse Fe3O4 Nanoparticles for Reduced Non-Specific Uptake by Macrophage Cells. *Adv. Mater.* **2007**, *19*, 3163.
(62) von Maltzahn, G.; Park, J. H.; Agrawal, A.; Bandaru, N. K.; Das, S. K.; Sailor, M. J.; Bhatia, S. N. Computationally Guided Photothermal Tumor Therapy Using Long-Circulating Gold Nanorod Antennas. *Cancer Res.* **2009**, *69*, 3892−3900.
(63) Koole, R.; van Schooneveld, M. M.; Hilhorst, J.; Castermans, K.; Cormode, D. P.; Strijkers, G. J.; Donega, C. D.; Vanmaekelbergh, D.; Griffioen, A. W.; Nicolay, K.; Fayad, Z. A.; Meijerink, A.; Mulder, W. J. M. Paramagnetic Lipid-Coated Silica Nanoparticles with a Fluorescent Quantum Dot Core: A New Contrast Agent Platform for Multimodality Imaging. *Bioconjugate Chem.* **2008**, *19*, 2471−2479.
(64) Ishida, T.; Ichihara, M.; Wang, X.; Yamamoto, K.; Kimura, J.; Majima, E.; Kiwada, H. Injection of PEGylated Liposomes in Rats Elicits PEG-Specific IgM, Which Is Responsible for Rapid Elimination of a Second Dose of PEGylated Liposomes. *J. Controlled Release* **2006**, *112*, 15−25.
(65) Wang, X. Y.; Ishida, T.; Kiwada, H. Anti-PEG IgM Elicited by Injection of Liposomes is Involved in the Enhanced Blood Clearance of a Subsequent Dose of PEGylated Liposomes. *J. Controlled Release* **2007**, *119*, 236−244.
(66) Ishida, T.; Wang, X.; Shimizu, T.; Nawata, K.; Kiwada, H. PEGylated Liposomes Elicit an Anti-PEG IgM Response in a T Cell-Independent Manner. *J. Controlled Release* **2007**, *122*, 349−355.
(67) Ishida, T.; Kiwada, H. Accelerated Blood Clearance (ABC) Phenomenon upon Repeated Injection of PEGylated Liposomes. *Int. J. Pharm.* **2008**, *354*, 56−62.
(68) Amoozgar, Z.; Yeo, Y. Recent Advances in Stealth Coating of Nanoparticle Drug Delivery Systems. *Wiley Interdiscip. Rev. Nanomed. Nanobiotechnol.* **2012**, *4*, 219−233.
(69) Mishra, S.; Webster, P.; Davis, M. E. PEGylation Significantly Affects Cellular Uptake and Intracellular Trafficking of Non-Viral Gene Delivery Particles. *Eur. J. Cell Biol.* **2004**, *83*, 97−111.
(70) Hatakeyama, H.; Akita, H.; Harashima, H. A Multifunctional Envelope Type Nano Device (MEND) for Gene Delivery to Tumours Based on the EPR Effect: a Strategy for Overcoming the PEG Dilemma. *Adv. Drug Delivery Rev.* **2011**, *63*, 152−160.
(71) Hamad, I.; Hunter, A. C.; Szebeni, J.; Moghimi, S. M. Poly(ethylene glycol)s Generate Complement Activation Products in Human Serum Through Increased Alternative Pathway Turnover and a MASP-2-Dependent Process. *Mol. Immunol.* **2008**, *46*, 225−232.
(72) Wolfrum, C.; Shi, S.; Jayaprakash, K. N.; Jayaraman, M.; Wang, G.; Pandey, R. K.; Rajeev, K. G.; Nakayama, T.; Charrise, K.; Ndungo, E. M.; Zimmermann, T.; Koteliansky, V.; Manoharan, M.; Stoffel, M. Mechanisms and Optimization of *in Vivo* Delivery of Lipophilic siRNAs. *Nat. Biotechnol.* **2007**, *25*, 1149−1157.
(73) Zhang, Z. H.; Cao, W. G.; Jin, H. L.; Lovell, J. F.; Yang, M.; Ding, L. L.; Chen, J.; Corbin, I.; Luo, Q. M.; Zheng, G. Biomimetic Nanocarrier for Direct Cytosolic Drug Delivery. *Angew. Chem., Int. Ed.* **2009**, *48*, 9171−9175.
(74) Yang, M.; Jin, H. L.; Chen, J. A.; Ding, L. L.; Ng, K. K.; Lin, Q. Y.; Lovell, J. F.; Zhang, Z. H.; Zheng, G. Efficient Cytosolic Delivery of siRNA Using HDL-Mimicking Nanoparticles. *Small* **2011**, *7*, 568−573.
(75) Lasagna-Reeves, C.; Gonzalez-Romero, D.; Barria, M. A.; Olmedo, I.; Clos, A.; Ramanujam, V. M. S.; Urayama, A.; Vergara, L.; Kogan, M. J.; Soto, C. Bioaccumulation and Toxicity of Gold Nanoparticles after Repeated Administration in Mice. *Biochem. Biophys. Res. Commun.* **2010**, *393*, 649−655.
(76) Chen, Y. S.; Hung, Y. C.; Liau, I.; Huang, G. S. Assessment of the *in Vivo* Toxicity of Gold Nanoparticles. *Nanoscale Res. Lett.* **2009**, *4*, 858−864.
(77) Anselmo, A. C.; Mitragotri, S. A Review of Clinical Translation of Inorganic Nanoparticles. *AAPS J.* **2015**, *17*, 1041−1054.
(78) Allen, T. M.; Cullis, P. R. Liposomal Drug Delivery Systems: from Concept to Clinical Applications. *Adv. Drug Delivery Rev.* **2013**, *65*, 36−48.
(79) Danhier, F.; Ansorena, E.; Silva, J. M.; Coco, R.; Le Breton, A.; Preat, V. PLGA-Based Nanoparticles: an Overview of Biomedical Applications. *J. Controlled Release* **2012**, *161*, 505−22.
(80) Kamaly, N.; Xiao, Z. Y.; Valencia, P. M.; Radovic-Moreno, A. F.; Farokhzad, O. C. Targeted Polymeric Therapeutic Nanoparticles: Design, Development and Clinical Translation. *Chem. Soc. Rev.* **2012**, *41*, 2971−3010.
(81) Gong, J.; Chen, M.; Zheng, Y.; Wang, S.; Wang, Y. Polymeric Micelles Drug Delivery System in Oncology. *J. Controlled Release* **2012**, *159*, 312−23.
(82) Yokoyama, M. Polymeric Micelles as Drug Carriers: Their Lights and Shadows. *J. Drug Target.* **2014**, *22*, 576−83.
(83) Cui, L. Y.; Lin, Q. Y.; Jin, C. S.; Jiang, W. L.; Huang, H.; Ding, L. L.; Muhanna, N.; Irish, J. C.; Wang, F.; Chen, J.; Zheng, G. A PEGylation-Free Biomimetic Porphyrin Nanoplatform for Personalized Cancer Theranostics. *ACS Nano* **2015**, *9*, 4484−4495.
(84) Ng, K. K.; Lovell, J. F.; Zheng, G. Lipoprotein-Inspired Nanoparticles for Cancer Theranostics. *Acc. Chem. Res.* **2011**, *44*, 1105−1113.
(85) Klibanov, A. L.; Maruyama, K.; Torchilin, V. P.; Huang, L. Amphipathic Polyethyleneglycols Effectively Prolong The Circulation Time of Liposomes. *FEBS Lett.* **1990**, *268*, 235−7.
(86) Allen, T. M.; Hansen, C.; Martin, F.; Redemann, C.; Yau-Young, A. Liposomes Containing Synthetic Lipid Derivatives of Poly(ethylene glycol) Show Prolonged Circulation Half-lives *in Vivo*. *Biochim. Biophys. Acta, Biomembr.* **1991**, *1066*, 29−36.
(87) Sanchez-Gaytan, B. L.; Fay, F.; Lobatto, M. E.; Tang, J.; Ouimet, M.; Kim, Y.; van der Staay, S. E.; van Rijs, S. M.; Priem, B.; Zhang, L.; Fisher, E. A.; Moore, K. J.; Langer, R.; Fayad, Z. A.; Mulder, W. J. HDL-Mimetic PLGA Nanoparticle to Target Atherosclerosis Plaque Macrophages. *Bioconjugate Chem.* **2015**, *26*, 443−51.
(88) Cormode, D. P.; Briley-Saebo, K. C.; Mulder, W. J. M.; Aguinaldo, J. G. S.; Barazza, A.; Ma, Y. Q.; Fisher, E. A.; Fayad, Z. A. An ApoA-I Mimetic Peptide High-Density-Lipoprotein-Based MRI Contrast Agent for Atherosclerotic Plaque Composition Detection. *Small* **2008**, *4*, 1437−1444.
(89) Hirsch, L. R.; Stafford, R. J.; Bankson, J. A.; Sershen, S. R.; Rivera, B.; Price, R. E.; Hazle, J. D.; Halas, N. J.; West, J. L. Nanoshell-Mediated Near-Infrared Thermal Therapy of Tumors under Magnetic Resonance Guidance. *Proc. Natl. Acad. Sci. U. S. A.* **2003**, *100*, 13549−13554.
(90) Gad, S. C.; Sharp, K. L.; Montgomery, C.; Payne, J. D.; Goodrich, G. P. Evaluation of the Toxicity of Intravenous Delivery of Auroshell Particles (Gold-Silica Nanoshells). *Int. J. Toxicol.* **2012**, *31*, 584−94.
(91) Schwartz, J. A.; Shetty, A. M.; Price, R. E.; Stafford, R. J.; Wang, J. C.; Uthamanthil, R. K.; Pham, K.; McNichols, R. J.; Coleman, C. L.; Payne, J. D. Feasibility Study of Particle-Assisted Laser Ablation of Brain Tumors in Orthotopic Canine Model. *Cancer Res.* **2009**, *69*, 1659−1667.

DOI: 10.1021/acsnano.5b07522
ACS Nano 2016, 10, 3015−3041

(92) Pilot Study of AuroLase(tm) Therapy in Refractory and/or Recurrent Tumors of the Head and Neck. https://clinicaltrials.gov/ct2/show/NCT00848042.
(93) Efficacy Study of AuroLase Therapy in Subjects with Primary and/or Metastatic Lung Tumors. https://www.clinicaltrials.gov/ct2/show/NCT01679470?term=NCT01679470&rank=1.
(94) Libutti, S. K.; Paciotti, G. F.; Byrnes, A. A.; Alexander, H. R.; Gannon, W. E.; Walker, M.; Seidel, G. D.; Yuldasheva, N.; Tamarkin, L. Phase I and Pharmacokinetic Studies of CYT-6091, a Novel PEGylated Colloidal Gold-rhTNF Nanomedicine. *Clin. Cancer Res.* **2010**, *16*, 6139−6149.
(95) Mclachlan, S. J.; Morris, M. R.; Lucas, M. A.; Fisco, R. A.; Eakins, M. N.; Fowler, D. R.; Scheetz, R. B.; Olukotun, A. Y. Phase-I Clinical-Evaluation of a New Iron-Oxide Mr Contrast Agent. *J. Magn. Reson. Imaging* **1994**, *4*, 301−307.
(96) Bellin, M. F.; Roy, C.; Kinkel, K.; Thoumas, D.; Zaim, S.; Vanel, D.; Tuchmann, C.; Richard, F.; Jacqmin, D.; Delcourt, A.; Challier, E.; Lebret, T.; Cluzel, P. Lymph Node Metastases: Safety and Effectiveness of MR Imaging with Ultrasmall Superparamagnetic Iron Oxide Particles - Initial Clinical Experience. *Radiology* **1998**, *207*, 799−808.
(97) Maier-Hauff, K.; Ulrich, F.; Nestler, D.; Niehoff, H.; Wust, P.; Thiesen, B.; Orawa, H.; Budach, V.; Jordan, A. Efficacy and Safety of Intratumoral Thermotherapy Using Magnetic Iron-Oxide Nanoparticles Combined with External Beam Radiotherapy on Patients with Recurrent Glioblastoma Multiforme. *J. Neuro-Oncol.* **2011**, *103*, 317−324.
(98) Hahn, P. F.; Stark, D. D.; Lewis, J. M.; Saini, S.; Elizondo, G.; Weissleder, R.; Fretz, C. J.; Ferrucci, J. T. First Clinical Trial of a New Superparamagnetic Iron Oxide for Use as an Oral Gastrointestinal Contrast Agent in MR Imaging. *Radiology* **1990**, *175*, 695−700.
(99) Spinowitz, B. S.; Schwenk, M. H.; Jacobs, P. M.; Bolton, W. K.; Kaplan, M. R.; Charytan, C.; Galler, M. The Safety and Efficacy of Ferumoxytol Therapy in Anemic Chronic Kidney Disease Patients. *Kidney Int.* **2005**, *68*, 1801−1807.
(100) Singh, A.; Patel, T.; Hertel, J.; Bernardo, M.; Kausz, A.; Brenner, L. Safety of Ferumoxytol in Patients With Anemia and CKD. *Am. J. Kidney Dis.* **2008**, *52*, 907−915.
(101) Phillips, E.; Penate-Medina, O.; Zanzonico, P. B.; Carvajal, R. D.; Mohan, P.; Ye, Y. P.; Humm, J.; Gonen, M.; Kalaigian, H.; Schoder, H.; Strauss, H. W.; Larson, S. M.; Wiesner, U.; Bradbury, M. S. Clinical Translation of an Ultrasmall Inorganic Optical-PET Imaging Nanoparticle Probe. *Sci. Transl. Med.* **2014**, *6*, 260ra149.
(102) Duivenvoorden, R.; Tang, J.; Cormode, D. P.; Mieszawska, A. J.; Izquierdo-Garcia, D.; Ozcan, C.; Otten, M. J.; Zaidi, N.; Lobatto, M. E.; van Rijs, S. M.; Priem, B.; Kuan, E. L.; Martel, C.; Hewing, B.; Sager, H.; Nahrendorf, M.; Randolph, G. J.; Stroes, E. S. G.; Fuster, V.; Fisher, E. A. A Statin-Loaded Reconstituted High-Density Lipoprotein Nanoparticle Inhibits Atherosclerotic Plaque Inflammation. *Nat. Commun.* **2014**, *5*, 3065.
(103) Argraves, K. M.; Gazzolo, P. J.; Groh, E. M.; Wilkerson, B. A.; Matsuura, B. S.; Twal, W. O.; Hammad, S. M.; Argraves, W. S. High Density Lipoprotein-Associated Sphingosine 1-Phosphate Promotes Endothelial Barrier Function. *J. Biol. Chem.* **2008**, *283*, 25074−25081.
(104) de Vrueh, R. L. A.; Rump, E. T.; van de Bilt, E.; van Veghel, R.; Balzarini, J.; Biessen, E. A. L.; van Berkel, T. J. C.; Bijsterbosch, M. K. Carrier-Mediated Delivery of 9-(2-phosphonylmethoxyethyl)adenine to Parenchymal Liver Cells: a Novel Therapeutic Approach for Hepatitis B. *Antimicrob. Agents Chemother.* **2000**, *44*, 477−483.
(105) Oda, M. N.; Hargreaves, P. L.; Beckstead, J. A.; Redmond, K. A.; van Antwerpen, R.; Ryan, R. O. Reconstituted High Density Lipoprotein Enriched with the Polyene Antibiotic Amphotericin B. *J. Lipid Res.* **2006**, *47*, 260−267.
(106) Zhang, X. B.; Chen, B. S. Recombinant High Density Lipoprotein Reconstituted with Apolipoprotein AI Cysteine Mutants as Delivery Vehicles for 10-Hydroxycamptothecin. *Cancer Lett.* **2010**, *298*, 26−33.
(107) Singh, A. T. K.; Evens, A. M.; Anderson, R. J.; Beckstead, J. A.; Sankar, N.; Sassano, A.; Bhalla, S.; Yang, S.; Platanias, L. C.; Forte, T. M.; Ryan, R. O.; Gordon, L. I. All Trans Retinoic Acid Nanodisks Enhance Retinoic Acid Receptor Mediated Apoptosis and Cell Cycle Arrest in Mantle Cell Lymphoma. *Br. J. Hamaetol.* **2010**, *150*, 158−169.
(108) Ghosh, M.; Singh, A. T. K.; Xu, W. W.; Sulchek, T.; Gordon, L. I.; Ryan, R. O. Curcumin Nanodisks: Formulation and Characterization. *Nanomedicine* **2011**, *7*, 162−167.
(109) Singh, A. T. K.; Ghosh, M.; Forte, T. M.; Ryan, R. O.; Gordon, L. I. Curcumin Nanodisk-Induced Apoptosis in Mantle Cell Lymphoma. *Leuk. Lymphoma* **2011**, *52*, 1537−1543.
(110) McConathy, W. J.; Nair, M. P.; Paranjape, S.; Mooberry, L.; Lacko, A. G. Evaluation of Synthetic/Reconstituted High-Density Lipoproteins as Delivery Vehicles for Paclitaxel. *Anti-Cancer Drugs* **2008**, *19*, 183−188.
(111) Mooberry, L. K.; Nair, M.; Paranjape, S.; McConathy, W. J.; Lacko, A. G. Receptor Mediated Uptake of Paclitaxel from a Synthetic High Density Lipoprotein Nanocarrier. *J. Drug Target.* **2010**, *18*, 53−58.
(112) Yuan, Y.; Wang, W. N.; Wang, B. L.; Zhu, H. Y.; Zhang, B. H.; Feng, M. Q. Delivery of Hydrophilic Drug Doxorubicin Hydrochloride-Targeted Liver Using ApoAI as Carrier. *J. Drug Target.* **2013**, *21*, 367−374.
(113) Weilhammer, D. R.; Blanchette, C. D.; Fischer, N. O.; Alam, S.; Loots, G. G.; Corzett, M.; Thomas, C.; Lychak, C.; Dunkle, A. D.; Ruitenberg, J. J.; Ghanekar, S. A.; Sant, A. J.; Rasley, A. The Use of Nanolipoprotein Particles to Enhance the Immunostimulatory Properties of Innate Immune Agonists Against Lethal Influenza Challenge. *Biomaterials* **2013**, *34*, 10305−10318.
(114) Feng, M. Q.; Cai, Q. S.; Shi, X. L.; Huang, H.; Zhou, P.; Guo, X. Recombinant High-Density Lipoprotein Complex as a Targeting System of Nosiheptide to Liver Cells. *J. Drug Target.* **2008**, *16*, 502−508.
(115) Kim, S. K.; Foote, M. B.; Huang, L. The Targeted Intracellular Delivery of Cytochrome C Protein to Tumors Using Lipid-Apolipoprotein Nanoparticles. *Biomaterials* **2012**, *33*, 3959−3966.
(116) Huang, C.; Jin, H. L.; Qian, Y.; Qi, S. H.; Luo, H. M.; Luo, Q. M.; Zhang, Z. H. Hybrid Melittin Cytolytic Peptide-Driven Ultrasmall Lipid Nanoparticles Block Melanoma Growth *in Vivo*. *ACS Nano* **2013**, *7*, 5791−5800.
(117) Fischer, N. O.; Rasley, A.; Corzett, M.; Hwang, M. H.; Hoeprich, P. D.; Blanchette, C. D. Colocalized Delivery of Adjuvant and Antigen Using Nanolipoprotein Particles Enhances the Immune Response to Recombinant Antigens. *J. Am. Chem. Soc.* **2013**, *135*, 2044−2047.
(118) Fischer, N. O.; Rasley, A.; Corzett, M.; Hwang, M. H.; Hoeprich, P. D.; Blanchette, C. D. Colocalized delivery of adjuvant and antigen using nanolipoprotein particles enhances the immune response to recombinant antigens. *J. Am. Chem. Soc.* **2013**, *135*, 2044−7.
(119) Nakayama, T.; Butler, J. S.; Sehgal, A.; Severgnini, M.; Racie, T.; Sharman, J.; Ding, F.; Morskaya, S. S.; Brodsky, J.; Tchangov, L.; Kosovrasti, V.; Meys, M.; Nechev, L.; Wang, G.; Peng, C. G.; Fang, Y. P.; Maier, M.; Rajeev, K. G.; Li, R.; Hettinger, J.; et al. Harnessing a Physiologic Mechanism for siRNA Delivery With Mimetic Lipoprotein Particles. *Mol. Ther.* **2012**, *20*, 1582−1589.
(120) Shahzad, M. M. K.; Mangala, L. S.; Han, H. D.; Lu, C. H.; Bottsford-Miller, J.; Nishimura, M.; Mora, E. M.; Lee, J. W.; Stone, R. L.; Pecot, C. V.; Thanapprapasr, D.; Roh, J. W.; Gaur, P.; Nair, M. P.; Park, Y. Y.; Sabnis, N.; Deavers, M. T.; Lee, J. S.; Ellis, L. M.; Lopez-Berestein, G.; et al. Targeted Delivery of Small Interfering RNA Using Reconstituted High-Density Lipoprotein Nanoparticles. *Neoplasia* **2011**, *13*, 309−U142.
(121) Kuwahara, H.; Nishina, K.; Yoshida, K.; Nishina, T.; Yamamoto, M.; Saito, Y.; Piao, W. Y.; Yoshida, M.; Mizusawa, H.; Yokota, T. Efficient *in Vivo* Delivery of siRNA into Brain Capillary Endothelial Cells along With Endogenous Lipoprotein. *Mol. Ther.* **2011**, *19*, 2213−2221.

DOI: 10.1021/acsnano.5b07522
ACS Nano 2016, 10, 3015−3041

(122) Libby, P.; Ridker, P. M.; Hansson, G. K. Progress and Challenges in Translating the Biology of Atherosclerosis. *Nature* **2011**, *473*, 317−325.
(123) Vanderwal, A. C.; Becker, A. E.; Vanderloos, C. M.; Das, P. K. Site of Intimal Rupture or Erosion of Thrombosed Coronary Atherosclerotic Plaques Is Characterized by an Inflammatory Process Irrespective of the Dominant Plaque Morphology. *Circulation* **1994**, *89*, 36−44.
(124) Weber, C.; Noels, H. Atherosclerosis: Current Pathogenesis and Therapeutic Options. *Nat. Med.* **2011**, *17*, 1410−1422.
(125) Zhang, W. L.; He, H. L.; Liu, J. P.; Wang, J.; Zhang, S. Y.; Zhang, S. S.; Wu, Z. M. Pharmacokinetics and Atherosclerotic Lesions Targeting Effects of Tanshinone IIA Discoidal and Spherical Biomimetic High Density Lipoproteins. *Biomaterials* **2013**, *34*, 306−319.
(126) Moulton, K. S.; Olsen, B. R.; Sonn, S.; Fukai, N.; Zurakowski, D.; Zeng, X. K. Loss of Collagen XVIII Enhances Neovascularization and Vascular Permeability in Atherosclerosis. *Circulation* **2004**, *110*, 1330−1336.
(127) Rader, D. J. Molecular regulation of HDL metabolism and function: implications for novel therapies. *J. Clin. Invest.* **2006**, *116*, 3090−100.
(128) Zhang, W. L.; Xiao, Y.; Liu, J. P.; Wu, Z. M.; Gu, X.; Xu, Y. M.; Lu, H. Structure and Remodeling Behavior of Drug-loaded High Density Lipoproteins and Their Aerosclerotic Plaque Targeting Mechanism in Foam Cell Model. *Int. J. Pharm.* **2011**, *419*, 314−321.
(129) Poelstra, K.; Prakash, J.; Beljaars, L. Drug Targeting to the Diseased Liver. *J. Controlled Release* **2012**, *161*, 188−197.
(130) Smith, J. S.; Xu, Z. L.; Byrnes, A. P. A Quantitative Assay for Measuring Clearance of Adenovirus Vectors by Kupffer Cells. *J. Virol. Methods* **2008**, *147*, 54−60.
(131) Wang, H. X.; Xiong, M. H.; Wang, Y. C.; Zhu, J.; Wang, J. N-acetylgalactosamine Functionalized Mixed Micellar Nanoparticles for Targeted Delivery of siRNA to Liver. *J. Controlled Release* **2013**, *166*, 106−114.
(132) Tian, Q.; Zhang, C. N.; Wang, X. H.; Wang, W.; Huang, W.; Cha, R. T.; Wang, C. H.; Yuan, Z.; Liu, M.; Wan, H. Y.; Tang, H. Glycyrrhetinic Acid-Modified Chitosan/Poly(ethylene glycol) Nanoparticles for Liver-Targeted Delivery. *Biomaterials* **2010**, *31*, 4748−4756.
(133) Hirata, K.; Maruyama, T.; Watanabe, H.; Maeda, H.; Nakajou, K.; Iwao, Y.; Ishima, Y.; Katsumi, H.; Hashida, M.; Otagiri, M. Genetically Engineered Mannosylated-Human Serum Albumin as a Versatile Carrier for Liver-Selective Therapeutics. *J. Controlled Release* **2010**, *145*, 9−16.
(134) Deng, Q.; Mancini-Bourgine, M.; Zhang, X. M.; Cumont, M. C.; Zhu, R.; Lone, Y. C.; Michel, M. L. Hepatitis B Virus As a Gene Delivery Vector Activating Foreign Antigenic T Cell Response that Abrogates Viral Expression in Mouse Models. *Hepatology* **2009**, *50*, 1380−1391.
(135) Giacca, M.; Zacchigna, S. Virus-Mediated Gene Delivery for Human Gene Therapy. *J. Controlled Release* **2012**, *161*, 377−388.
(136) Rensen, P. C. N.; de Vrueh, R. L. A.; Kuiper, J.; Bijsterbosch, M. K.; Biessen, E. A. L.; van Berkel, T. J. C. Recombinant Lipoproteins: Lipoprotein-Like Lipid Particles for Drug Targeting. *Adv. Drug Delivery Rev.* **2001**, *47*, 251−276.
(137) Gullotti, E.; Yeo, Y. Extracellularly Activated Nanocarriers: A New Paradigm of Tumor Targeted Drug Delivery. *Mol. Pharmaceutics* **2009**, *6*, 1041−1051.
(138) Eisenberg, S.; Windmueller, H. G.; Levy, R. I. Metabolic Fate of Rat and Human Lipoprotein Apoproteins in the Rat. *J. Lipid Res.* **1973**, *14*, 446−58.
(139) Pluen, A.; Boucher, Y.; Ramanujan, S.; McKee, T. D.; Gohongi, T.; di Tomaso, E.; Brown, E. B.; Izumi, Y.; Campbell, R. B.; Berk, D. A.; Jain, R. K. Role of Tumor-Host Interactions in Interstitial Diffusion of Macromolecules: Cranial vs. Subcutaneous Tumors. *Proc. Natl. Acad. Sci. U. S. A.* **2001**, *98*, 4628−4633.
(140) Siperstein, M. D. Role of Cholesterogenesis and Isoprenoid Synthesis in DNA-Replication and Cell-Growth. *J. Lipid Res.* **1984**, *25*, 1462−1468.
(141) Hynds, S. A.; Welsh, J.; Stewart, J. M.; Jack, A.; Soukop, M.; Mcardle, C. S.; Calman, K. C.; Packard, C. J.; Shepherd, J. Low-Density Lipoprotein Metabolism in Mice with Soft-Tissue Tumors. *Biochim. Biophys. Acta, Lipids Lipid Metab.* **1984**, *795*, 589−595.
(142) Vitols, S.; Norgren, S.; Juliusson, G.; Tatidis, L.; Luthman, H. Multilevel Regulation of Low-Density-Lipoprotein Receptor and 3-Hydroxy-3-Methylglutaryl Coenzyme-a Reductase Gene-Expression in Normal and Leukemic-Cells. *Blood* **1994**, *84*, 2689−2698.
(143) Pussinen, P. J.; Karten, B.; Wintersperger, A.; Reicher, H.; McLean, M.; Malle, E.; Sattler, W. The Human Breast Carcinoma Cell Line HBL-100 Acquires Exogenous Cholesterol from High-Density Lipoprotein *via* CLA-1 (CD-36 and LIMPII Analogous 1)-Mediated Selective Cholesteryl Ester Uptake. *Biochem. J.* **2000**, *349*, 559−566.
(144) Imachi, H.; Murao, K.; Sayo, Y.; Hosokawa, H.; Sato, M.; Niimi, M.; Kobayashi, S.; Miyauchi, A.; Ishida, T.; Takahara, J. Evidence for a Potential Role for HDL as an Important Source of Cholesterol in Human Adrenocortical Tumors *via* the CLA-1 Pathway. *Endocr. J.* **1999**, *46*, 27−34.
(145) Leon, C. G.; Locke, J. A.; Adomat, H. H.; Etinger, S. L.; Twiddy, A. L.; Neumann, R. D.; Nelson, C. C.; Guns, E. S.; Wasan, K. M. Alterations in Cholesterol Regulation Contribute to the Production of Intratumoral Androgens During Progression to Castration-Resistant Prostate Cancer in a Mouse Xenograft Model. *Prostate* **2010**, *70*, 390−400.
(146) Zhang, Z. H.; Chen, J.; Ding, L. L.; Jin, H. L.; Lovell, J. F.; Corbin, I. R.; Cao, W. G.; Lo, P. C.; Yang, M.; Tsao, M. S.; Luo, Q. M.; Zheng, G. HDL-Mimicking Peptide-Lipid Nanoparticles with Improved Tumor Targeting. *Small* **2010**, *6*, 430−437.
(147) Chen, W.; Jarzyna, P. A.; van Tilborg, G. A. F.; Nguyen, V. A.; Cormode, D. P.; Klink, A.; Griffioen, A. W.; Randolph, G. J.; Fisher, E. A.; Mulder, W. J. M.; Fayad, Z. A. RGD Peptide Functionalized and Reconstituted High-Density Lipoprotein Nanoparticles as a Versatile and Multimodal Tumor Targeting Molecular Imaging Probe. *FASEB J.* **2010**, *24*, 1689−1699.
(148) Corbin, I. R.; Ng, K. K.; Ding, L. L.; Jurisicova, A.; Zheng, G. Near-Infrared Fluorescent Imaging of Metastatic Ovarian Cancer Using Folate Receptor-Targeted High-Density Lipoprotein Nanocarriers. *Nanomedicine* **2013**, *8*, 875−890.
(149) Corbin, I. R.; Chen, J.; Cao, W.; Li, H.; Lund-Katz, S.; Zheng, G. Enhanced Cancer-Targeted Delivery Using Engineered High-Density Lipoprotein-Based Nanocarriers. *J. Biomed. Nanotechnol.* **2007**, *3*, 367−376.
(150) Mellman, I.; Coukos, G.; Dranoff, G. Cancer Immunotherapy Comes of Age. *Nature* **2011**, *480*, 480−9.
(151) Joshi, M. D.; Unger, W. J.; Storm, G.; van Kooyk, Y.; Mastrobattista, E. Targeting Tumor Antigens to Dendritic Cells Using Particulate Carriers. *J. Controlled Release* **2012**, *161*, 25−37.
(152) Beutler, B. Inferences, 1uestions and Possibilities in Toll-like Receptor Signalling. *Nature* **2004**, *430*, 257−263.
(153) Lawton, J. A.; Ghosh, P. Novel Therapeutic Strategies Based on Toll-Like Receptor Signaling. *Curr. Opin. Chem. Biol.* **2003**, *7*, 446−451.
(154) Sahdev, P.; Ochyl, L. J.; Moon, J. J. Biomaterials for Nanoparticle Vaccine Delivery Systems. *Pharm. Res.* **2014**, *31*, 2563−2582.
(155) Wilson, J. T.; Keller, S.; Manganiello, M. J.; Cheng, C.; Lee, C. C.; Opara, C.; Convertine, A.; Stayton, P. S. pH-Responsive Nanoparticle Vaccines for Dual-Delivery of Antigens and Immunostimulatory Oligonucleotides. *ACS Nano* **2013**, *7*, 3912−3925.
(156) Yuba, E.; Harada, A.; Sakanishi, Y.; Watarai, S.; Kono, K. A Liposome-Based Antigen Delivery System Using pH-Sensitive Fusogenic Polymers for Cancer Immunotherapy. *Biomaterials* **2013**, *34*, 3042−3052.
(157) Hamdy, S.; Haddadi, A.; Hung, R. W.; Lavasanifar, A. Targeting Dendritic Cells with Nano-Particulate PLGA Cancer Vaccine Formulations. *Adv. Drug Delivery Rev.* **2011**, *63*, 943−955.

DOI: 10.1021/acsnano.5b07522
ACS Nano 2016, 10, 3015−3041

(158) Fischer, N. O.; Blanchette, C.; Rasley, A. Enhancing the Efficacy of Innate Immune Agonists: Could Nanolipoprotein Particles Hold the Key? *Nanomedicine* **2014**, *9*, 369−372.
(159) Kuai, R. Ochyl, L. J.; Schwendeman, A.; Moon, J. J. Lipid-Based Nanoparticles for Vaccine Applications. In *Biomedical Engineering: Frontier Research and Converging Technologies*; Jo, H., Jun, H. W., Shin, J., Lee, S.-H., Eds.; Springer, 2016; Vol. *9*, pp 177−197.
(160) Bachmann, M. F.; Jennings, G. T. Vaccine Delivery: a Matter of Size, Geometry, Kinetics and Molecular Patterns. *Nat. Rev. Immunol.* **2010**, *10*, 787−796.
(161) Krishnamachari, Y.; Salem, A. K. Innovative Strategies for Co-delivering Antigens and CpG Oligonucleotides. *Adv. Drug Delivery Rev.* **2009**, *61*, 205−217.
(162) Mutwiri, G. K.; Nichani, A. K.; Babiuk, S.; Babiuk, L. A. Strategies for Enhancing the Immunostimulatory Effects of CpG Oligodeoxynucleotides. *J. Controlled Release* **2004**, *97*, 1−17.
(163) Hogquist, K. A.; Baldwin, T. A.; Jameson, S. C. Central Tolerance: Learning Self-Control in the Thymus. *Nat. Rev. Immunol.* **2005**, *5*, 772−782.
(164) Mueller, D. L. Mechanisms Maintaining Peripheral Tolerance. *Nat. Immunol.* **2010**, *11*, 21−27.
(165) Norata, G. D.; Pirillo, A.; Ammirati, E.; Catapano, A. L. Emerging role of High Density Lipoproteins as a Player in the Immune System. *Atherosclerosis* **2012**, *220*, 11−21.
(166) Blaho, V. A.; Galvani, S.; Engelbrecht, E.; Liu, C.; Swendeman, S. L.; Kono, M.; Proia, R. L.; Steinman, L.; Han, M. H.; Hla, T. HDL-Bound Sphingosine-1-Phosphate Restrains Lymphopoiesis and Neuroinflammation. *Nature* **2015**, *523*, 342−346.
(167) Hatch, F. T. Practical Methods for Plasma Lipoprotein Analysis. *Advances in Lipid Research*; Elsevier, 1968; Vol. *6*, pp 1−68.
(168) van den Elzen, P.; Garg, S.; Leon, L.; Brigl, M.; Leadbetter, E. A.; Gumperz, J. E.; Dascher, C. C.; Cheng, T. Y.; Sacks, F. M.; Illarionov, P. A.; Besra, G. S.; Kent, S. C.; Moody, D. B.; Brenner, M. B. Apolipoprotein-Mediated Pathways of Lipid Antigen Presentation. *Nature* **2005**, *437*, 906−910.
(169) Kim, Y.; Fay, F.; Cormode, D. P.; Sanchez-Gaytan, B. L.; Tang, J.; Hennessy, E. J.; Ma, M. M.; Moore, K.; Farokhzad, O. C.; Fisher, E. A.; Mulder, W. J. M.; Langer, R.; Fayad, Z. A. Single Step Reconstitution of Multifunctional High-Density Lipoprotein-Derived Nanomaterials Using Microfluidics. *ACS Nano* **2013**, *7*, 9975−9983.
(170) Rudman, D.; Hollins, B.; Bixler, T. J.; Mostelle, Rc Transport of Drugs, Hormones and Fatty-Acids in Lipemic Serum. *J. Pharmacol. Exp. Ther.* **1972**, *180*, 797.
(171) Counsell, R. E.; Pohland, R. C. Lipoproteins as Potential Site-Specific Delivery Systems for Diagnostic and Therapeutic Agents. *J. Med. Chem.* **1982**, *25*, 1115−1120.
(172) Goldstein, J. L.; Brown, M. S. Regulation of the Mevalonate Pathway. *Nature* **1990**, *343*, 425−430.
(173) Lefer, D. J. Statins as Potent Anti-Inflammatory Drugs. *Circulation* **2002**, *106*, 2041−2042.
(174) Kwak, B.; Mulhaupt, F.; Myit, S.; Mach, F. Statins as a Newly Recognized Type of Immunomodulator. *Nat. Med.* **2000**, *6*, 1399−1402.
(175) Armitage, J. The Safety of Statins in Clinical Practice. *Lancet* **2007**, *370*, 1781−1790.
(176) Nicoll, A. J.; Colledge, D. L.; Toole, J. J.; Angus, P. W.; Smallwood, R. A.; Locarnini, S. A. Inhibition of Duck Hepatitis B Virus Replication by 9-(2-phosphonylmethoxyethyl)adenine, an Acyclic Phosphonate Nucleoside Analogue. *Antimicrob. Agents Chemother.* **1998**, *42*, 3130−3135.
(177) Yokota, T.; Mochizuki, S.; Konno, K.; Mori, S.; Shigeta, S.; Declercq, E. Inhibitory Effects of Selected Antiviral Compounds on Human Hepatitis-B Virus-DNA Synthesis. *Antimicrob. Agents Chemother.* **1991**, *35*, 394−397.
(178) Naesens, L.; Balzarini, J.; Declercq, E. Pharmacokinetics in Mice of the Antiretrovirus Agent 9-(2-Phosphonylmethoxyethyl)-Adenine. *Drug Metab. Dispos.* **1992**, *20*, 747−752.
(179) Wall, M. E. Camptothecin and Taxol: Discovery to Clinic. *Med. Res. Rev.* **1998**, *18*, 299−314.
(180) Wang, A.; Li, S. Hydroxycamptothecin-Loaded Nanoparticles Enhance Target Drug Delivery and Anticancer Effect. *BMC Biotechnol.* **2008**, *8*, 46.
(181) Sattler, K.; Levkau, B. Sphingosine-1-Phosphate as a Mediator of High-Density Lipoprotein Effects in Cardiovascular Protection. *Cardiovasc. Res.* **2009**, *82*, 201−211.
(182) Manning, M. C.; Chou, D. K.; Murphy, B. M.; Payne, R. W.; Katayama, D. S. Stability of Protein Pharmaceuticals: An Update. *Pharm. Res.* **2010**, *27*, 544−575.
(183) Tabata, Y.; Ikada, Y. Protein Release from Gelatin Matrices. *Adv. Drug Delivery Rev.* **1998**, *31*, 287−301.
(184) Shah, A. S.; Tan, L.; Long, J. L.; Davidson, W. S. Thematic Review Series: High Density Lipoprotein Structure, Function, and Metabolism Proteomic Diversity of High Density Lipoproteins: Our Emerging Understanding of Its Importance in Lipid Transport and Beyond. *J. Lipid Res.* **2013**, *54*, 2575−2585.
(185) Benazet, F.; Cartier, M.; Florent, J.; Godard, C.; Jung, G.; Lunel, J.; Mancy, D.; Pascal, C.; Renaut, J.; Tarridec, P.; Theilleux, J.; Tissier, R.; Dubost, M.; Ninet, L. Nosiheptide, a Sulfur-Containing Peptide Antibiotic Isolated from Streptomyces-Actuosus 40037. *Experientia* **1980**, *36*, 414−416.
(186) Papo, N.; Shai, Y. Host Defense Peptides as New Weapons in Cancer Treatment. *Cell. Mol. Life Sci.* **2005**, *62*, 784−790.
(187) Liu, S. J.; Yu, M.; He, Y.; Xiao, L.; Wang, F.; Song, C. C.; Sun, S. H.; Ling, C. Q.; Xu, Z. H. Melittin Prevents Liver Cancer Cell Metastasis through Inhibition of the Rac1-Dependent Pathway. *Hepatology* **2008**, *47*, 1964−1973.
(188) Aguilar, J. C.; Rodriguez, E. G. Vaccine Adjuvants Revisited. *Vaccine* **2007**, *25*, 3752−3762.
(189) Xu, Z. H.; Ramishetti, S.; Tseng, Y. C.; Guo, S. T.; Wang, Y. H.; Huang, L. Multifunctional Nanoparticles Co-delivering Trp2 Peptide and CpG Adjuvant Induce Potent Cytotoxic T-Lymphocyte Response Against Melanoma and Its Lung Metastasis. *J. Controlled Release* **2013**, *172*, 259−265.
(190) Molino, N. M.; Anderson, A. K. L.; Nelson, E. L.; Wang, S. W. Biomimetic Protein Nanoparticles Facilitate Enhanced Dendritic Cell Activation and Cross-Presentation. *ACS Nano* **2013**, *7*, 9743−9752.
(191) Fischer, N. O.; Infante, E.; Ishikawa, T.; Blanchette, C. A.; Bourne, N.; Hoeprich, P. D.; Mason, P. W. Conjugation to Nickel-Chelating Nanolipoprotein Particles Increases the Potency and Efficacy of Subunit Vaccines to Prevent West Nile Encephalitis. *Bioconjugate Chem.* **2010**, *21*, 1018−1022.
(192) Fischer, N. O.; Blanchette, C. D.; Chromy, B. A.; Kuhn, E. A.; Segelke, B. W.; Corzett, M.; Bench, G.; Mason, P. W.; Hoeprich, P. D. Immobilization of His-Tagged Proteins on Nickel-Chelating Nanolipoprotein Particles. *Bioconjugate Chem.* **2009**, *20*, 460−465.
(193) Gomes-da-Silva, L. C.; Fonseca, N. A.; Moura, V.; de Lima, M. C. P.; Simoes, S.; Moreira, J. N. Lipid-Based Nanoparticles for siRNA Delivery in Cancer Therapy: Paradigms and Challenges. *Acc. Chem. Res.* **2012**, *45*, 1163−1171.
(194) Eder, P. S.; DeVine, R. J.; Dagle, J. M.; Walder, J. A. Substrate Specificity and Kinetics of Degradation of Antisense Oligonucleotides by a 3′ Exonuclease in Plasma. *Antisense Res. Dev.* **1991**, *1*, 141−51.
(195) Kennedy, S.; Wang, D.; Ruvkun, G. A Conserved siRNA-Degrading RNase Negatively Regulates RNA Interference in C-elegans. *Nature* **2004**, *427*, 645−649.
(196) Guo, S. T.; Huang, L. Nanoparticles Escaping RES and Endosome: Challenges for siRNA Delivery for Cancer Therapy. *J. Nanomater.* **2011**, *2011*, 1.
(197) Chendrimada, T. P.; Gregory, R. I.; Kumaraswamy, E.; Norman, J.; Cooch, N.; Nishikura, K.; Shiekhattar, R. TRBP Recruits the Dicer Complex to Ago2 for MicroRNA Processing and Gene Silencing. *Nature* **2005**, *436*, 740−744.
(198) Matranga, C.; Tomari, Y.; Shin, C.; Bartel, D. P.; Zamore, P. D. Passenger-Strand Cleavage Facilitates Assembly of siRNA into Ago2-Containing RNAi Enzyme Complexes. *Cell* **2005**, *123*, 607−620.
(199) Behlke, M. A. Chemical Modification of siRNAs for *in Vivo* Use. *Oligonucleotides* **2008**, *18*, 305−319.

DOI: 10.1021/acsnano.5b07522
ACS Nano 2016, 10, 3015−3041

(200) Frank-Kamenetsky, M.; Grefhorst, A.; Anderson, N. N.; Racie, T. S.; Bramlage, B.; Akinc, A.; Butler, D.; Charisse, K.; Dorkin, R.; Fan, Y.; Gamba-Vitalo, C.; Hadwiger, P.; Jayaraman, M.; John, M.; Jayaprakash, K. N.; Maier, M.; Nechev, L.; Rajeev, K. G.; Read, T.; Rohl, I.; et al. Therapeutic RNAi Targeting PCSK9 Acutely Lowers Plasma Cholesterol in Rodents and LDL Cholesterol in Nonhuman Primates. *Proc. Natl. Acad. Sci. U. S. A.* **2008**, *105*, 11915−11920.
(201) Higuchi, Y.; Kawakami, S.; Hashida, M. Strategies for *in Vivo* Delivery of siRNAs Recent Progress. *BioDrugs* **2010**, *24*, 195−205.
(202) Singha, K.; Namgung, R.; Kim, W. J. Polymers in Small-Interfering RNA Delivery. *Nucleic Acid Ther.* **2011**, *21*, 133−147.
(203) Li, S. D.; Huang, L. Nanoparticles Evading the Reticuloendothelial System: Role of the Supported Bilayer. *Biochim. Biophys. Acta, Biomembr.* **2009**, *1788*, 2259−2266.
(204) Heyes, J.; Palmer, L.; Bremner, K.; MacLachlan, I. Cationic Lipid Saturation Influences Intracellular Delivery of Encapsulated Nucleic Acids. *J. Controlled Release* **2005**, *107*, 276−287.
(205) Meade, B. R.; Dowdy, S. F. Exogenous siRNA Delivery Using Peptide Transduction Domains/Cell Penetrating Peptides. *Adv. Drug Delivery Rev.* **2007**, *59*, 134−140.
(206) Tabet, F.; Vickers, K. C.; Torres, L. F. C.; Wiese, C. B.; Shoucri, B. M.; Lambert, G.; Catherinet, C.; Prado-Lourenco, L.; Levin, M. G.; Thacker, S.; Sethupathy, P.; Barter, P. J.; Remaley, A. T.; Rye, K. A. HDL-Transferred MicroRNA-223 Regulates ICAM-1 Expression in Endothelial Cells. *Nat. Commun.* **2014**, *5*, 3292.
(207) Soutschek, J.; Akinc, A.; Bramlage, B.; Charisse, K.; Constien, R.; Donoghue, M.; Elbashir, S.; Geick, A.; Hadwiger, P.; Harborth, J.; John, M.; Kesavan, V.; Lavine, G.; Pandey, R. K.; Racie, T.; Rajeev, K. G.; Rohl, I.; Toudjarska, I.; Wang, G.; Wuschko, S.; et al. Therapeutic Silencing of an Endogenous Gene by Systemic Administration of Modified siRNAs. *Nature* **2004**, *432*, 173−178.
(208) Brown, M. S.; Goldstein, J. L. The Receptor Model for Transport of Cholesterol in Plasma. *Ann. N. Y. Acad. Sci.* **1985**, *454*, 178−182.
(209) Lin, Q. Y.; Chen, J.; Jin, H. L.; Ng, K. K.; Yang, M.; Cao, W. G.; Ding, L. L.; Zhang, Z. H.; Zheng, G. Efficient Systemic Delivery of siRNA by Using High-Density Lipoprotein-Mimicking Peptide Lipid Nanoparticles. *Nanomedicine* **2012**, *7*, 1813−1825.
(210) Ding, Y.; Wang, W.; Feng, M. Q.; Wang, Y.; Zhou, J. P.; Ding, X. F.; Zhou, X.; Liu, C. Y.; Wang, R. N.; Zhang, Q. A Biomimetic Nanovector-Mediated Targeted Cholesterol-Conjugated siRNA Delivery for Tumor Gene Therapy. *Biomaterials* **2012**, *33*, 8893−8905.
(211) Glickson, J. D.; Lund-Katz, S.; Zhou, R.; Choi, H.; Chen, I. W.; Li, H.; Corbin, I.; Popov, A. V.; Cao, W. G.; Song, L. P.; Qi, C. Z.; Marotta, D.; Nelson, D. S.; Chen, J.; Chance, B.; Zheng, G. Lipoprotein Nanoplatform for Targeted Delivery of Diagnostic and Therapeutic Agents. *Molecular Imaging* **2008**, *7*, 101−110.
(212) Frias, J. C.; Williams, K. J.; Fisher, E. A.; Fayad, Z. A. Recombinant HDL-Like Nanoparticles: A Specific Contrast Agent for MRI of Atherosclerotic Plaques. *J. Am. Chem. Soc.* **2004**, *126*, 16316−16317.
(213) Skajaa, T.; Cormode, D. P.; Jarzyna, P. A.; Delshad, A.; Blachford, C.; Barazza, A.; Fisher, E. A.; Gordon, R. E.; Fayad, Z. A.; Mulder, W. J. M. The Biological Properties of Iron Oxide Core High-Density Lipoprotein in Experimental Atherosclerosis. *Biomaterials* **2011**, *32*, 206−213.
(214) Cao, W. G.; Ng, K. K.; Corbin, I.; Zhang, Z. H.; Ding, L. L.; Chen, J.; Zheng, G. Synthesis and Evaluation of a Stable Bacteriochlorophyll-Analog and Its Incorporation into High-Density Lipoprotein Nanoparticles for Tumor Imaging. *Bioconjugate Chem.* **2009**, *20*, 2023−2031.
(215) Lin, Q. Y.; Chen, J.; Ng, K. K.; Cao, W. G.; Zhang, Z. H.; Zheng, G. Imaging the Cytosolic Drug Delivery Mechanism of HDL-Like Nanoparticles. *Pharm. Res.* **2014**, *31*, 1438−1449.
(216) Redondo, S.; Martinez-Gonzalez, J.; Urraca, C.; Tejerina, T. Emerging Therapeutic Strategies to Enhance HDL Function. *Lipids Health Dis.* **2011**, *10*, 175.
(217) Lundqvist, M.; Stigler, J.; Elia, G.; Lynch, I.; Cedervall, T.; Dawson, K. A. Nanoparticle Size and Surface Properties Determine the Protein Corona with Possible Implications for Biological Impacts. *Proc. Natl. Acad. Sci. U. S. A.* **2008**, *105*, 14265−14270.
(218) Ichikawa, K.; Takeuchi, Y.; Yonezawa, S.; Hikita, T.; Kurohane, K.; Namba, Y.; Oku, N. Antiangiogenic Photodynamic Therapy (PDT) Using Visudyne Causes Effective Suppression of Tumor Growth. *Cancer Lett.* **2004**, *205*, 39−48.
(219) Wang, H.; Eckel, R. H. What Are Lipoproteins Doing in the Brain? *Trends Endocrinol. Metab.* **2014**, *25*, 8−14.
(220) Sochaj, A. M.; Swiderska, K. W.; Otlewski, J. Current Methods for the Synthesis of Homogeneous Antibody-Drug Conjugates. *Biotechnol. Adv.* **2015**, *33*, 775−84.
(221) Morin, E. E.; Guo, L.; Schwendeman, A.; Li, X. HDL in Sepsis − Risk Factor and Therapeutic Approach. *Front. Pharmacol.* **2015**, *6*, 9.
(222) Subramanian, C.; Kuai, R.; Zhu, Q.; White, P.; Moon, J. J.; Schwendeman, A.; Cohen, M. S. Synthetic High-Density Lipoprotein Nanoparticles: A Novel Therapeutic Strategy for Adrenocortical Carcinomas. *Surgery* **2016**, *159*, 284−95.
(223) Song, Q. X.; Huang, M.; Yao, L.; Wang, X. L.; Gu, X.; Chen, J.; Chen, J.; Huang, J. L.; Hu, Q. Y.; Kang, T.; Rong, Z. X.; Qi, H.; Zheng, G.; Chen, H. Z.; Gao, X. L. Lipoprotein-Based Nanoparticles Rescue the Memory Loss of Mice with Alzheimer's Disease by Accelerating the Clearance of Amyloid-Beta. *ACS Nano* **2014**, *8*, 2345−2359.
(224) Huang, M.; Hu, M.; Song, Q.; Song, H.; Huang, J.; Gu, X.; Wang, X.; Chen, J.; Kang, T.; Feng, X.; Jiang, D.; Zheng, G.; Chen, H.; Gao, X. GM1-Modified Lipoprotein-like Nanoparticle: Multifunctional Nanoplatform for the Combination Therapy of Alzheimer's Disease. *ACS Nano* **2015**, *9*, 10801−16.

DOI: 10.1021/acsnano.5b07522
ACS Nano 2016, 10, 3015−3041